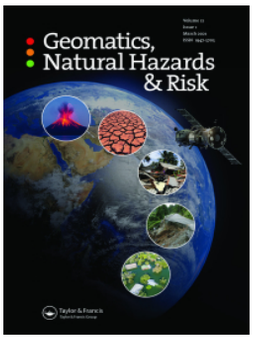

Geomatics, Natural Hazards and Risk

ISSN: (Print) (Online) Journal homepage: www.tandfonline.com/journals/tgnh20

Inventory and GLOF susceptibility of glacial lakes in Chenab basin, Western Himalaya

Suresh Das, Soumik Das, Sandip Tanu Mandal, Milap Chand Sharma & Raaj Ramsankaran

To cite this article: Suresh Das, Soumik Das, Sandip Tanu Mandal, Milap Chand Sharma & Raaj Ramsankaran (2024) Inventory and GLOF susceptibility of glacial lakes in Chenab basin, Western Himalaya, Geomatics, Natural Hazards and Risk, 15:1, 2356216, DOI: 10.1080/19475705.2024.2356216

To link to this article: https://doi.org/10.1080/19475705.2024.2356216

© 2024 The Author(s). Published by Informa UK Limited, trading as Taylor & Francis Group.

View supplementary material

Published online: 25 May 2024.

Submit your article to this journal

Article views: 1264

View related articles

View Crossmark data

Full Terms & Conditions of access and use can be found at
https://www.tandfonline.com/action/journalInformation?journalCode=tgnh20

GEOMATICS, NATURAL HAZARDS AND RISK
2024, VOL. 15, NO. 1, 2356216
https://doi.org/10.1080/19475705.2024.2356216

Taylor & Francis
Taylor & Francis Group

OPEN ACCESS Check for updates

Inventory and GLOF susceptibility of glacial lakes in Chenab basin, Western Himalaya

Suresh Das[a,b], Soumik Das[b], Sandip Tanu Mandal[b,c], Milap Chand Sharma[b] and RAAJ Ramsankaran[a]

[a]Hydro-Remote Sensing Applications (H-RSA) Group, Department of Civil Engineering, Indian Institute of Technology Bombay, Powai, India; [b]Centre for the Study of Regional Development, Jawaharlal Nehru University, New Delhi, India; [c]Mobius Foundation, New Delhi, India

ABSTRACT

Global warming causes glacial mass loss, leading to the growth of high-mountain glacial lakes. The presence of glacial lakes poses a significant threat to downstream communities, as they can produce destructive Glacial Lake Outburst Floods (GLOFs). Timely basin-scale inventory and GLOF susceptibility assessments are crucial, considering past GLOF events in the Himalayan region. Here, an updated inventory of glacial lakes in the Chenab basin, Western Himalayas was generated based on Sentinel-2 datasets for 2022. We assessed temporal changes and GLOF susceptibility for glacial lakes ($>0.05\,km^2$) through a multi-criteria based Analytical Hierarchical Process, classifying them into low, medium, high, and very high susceptibility classes. The results reveal 419 lakes ($>0.001\,km^2$; $9.97 \pm 0.67\,km^2$) in the basin in 2022. Glacial lakes ($>0.05\,km^2$) area increased by ~75%, from 3.92 ± 0.58 to $6.86 \pm 0.25\,km^2$ during 1990–2022. Of the 42 lakes ($>0.05\,km^2$) evaluated, four showed very high GLOF susceptibility. The study emphasizes the impact of local geomorphology and glacier-lake interaction under warming climate, likely to increase the GLOF susceptibility in the region. Regular monitoring and detailed fieldwork for these susceptible lakes are crucial for early warning and disaster risk reduction for downstream communities.

ARTICLE HISTORY
Received 25 January 2024
Accepted 12 May 2024

KEYWORDS
Glacial lakes; Glacial lake outburst flood; analytical hierarchical process; remote sensing; Chenab basin; Himalaya

CONTACT Suresh Das sureshdas088@gmail.com, suresh41_ssf@jnu.ac.in; RAAJ Ramsankaran ramsankaran@civil.iitb.ac.in

Supplemental data for this article can be accessed online at https://doi.org/10.1080/19475705.2024.2356216.

© 2024 The Author(s). Published by Informa UK Limited, trading as Taylor & Francis Group.
This is an Open Access article distributed under the terms of the Creative Commons Attribution-NonCommercial License (http://creativecommons.org/licenses/by-nc/4.0/), which permits unrestricted non-commercial use, distribution, and reproduction in any medium, provided the original work is properly cited. The terms on which this article has been published allow the posting of the Accepted Manuscript in a repository by the author(s) or with their consent.

GRAPHICAL ABSTRACT

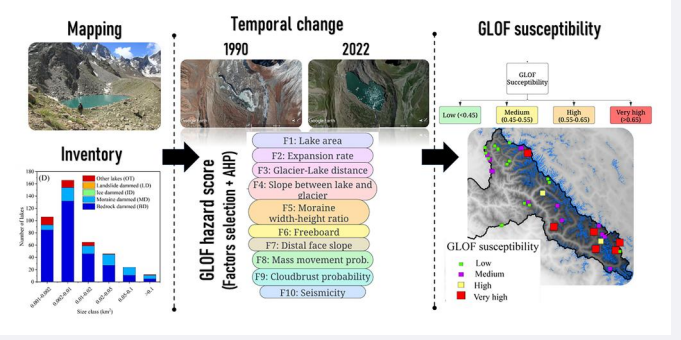

HIGHLIGHTS

- We present an improved inventory and GLOF susceptibility of glacial lakes for the Chenab basin, Western Himalaya.
- We mapped 419 lakes (>0.001 km^2) with a total area of 9.97 ± 0.67 km^2 as of 2022, much higher than previously reported.
- Glacial lake area increased by ~75% during 1990–2022.
- Four, three, and seven lakes are classified into the very high, high, and medium GLOF susceptible categories, respectively.
- Local geomorphology (i.e. avalanche, rockfall) and pronounced glacier-lake interaction under warming climate likely increase GLOF probability in the region.

1. Introduction

Climate change has already adversely affected the glaciated regions across the globe including in the Himalayas (Immerzeel et al. 2010). Recession and mass loss of glaciers in the Himalayan region have resulted in a rapid increase in the number and area of glacial lakes (Zhang et al. 2015; Wang et al. 2020a; Nie et al. 2021; Zheng et al. 2021). Glacial lakes often form due to damming by unstable and unconsolidated materials from the adjacent valley floors and glacier deposits (Carrivick and Tweed 2013; Westoby et al. 2014a; Tweed and Carrivick 2015; Linsbauer et al. 2016). Glacial lake outburst floods (GLOFs) comprise abrupt release and downstream movement of water and sediment from naturally dammed meltwater lakes (Allen et al. 2019; Fischer et al. 2021). GLOFs may cause catastrophic flash floods in the downstream areas and result in loss of lives and infrastructure (Westoby et al. 2014a; Das et al. 2015). Increasing population pressure and the growth of various anthropogenic activities (i.e. road construction, hydropower projects, and agricultural activities) increase exposure to probable GLOF (ICIMOD 2011). Therefore, frequent multi-temporal mapping and monitoring of glacial lakes is the initial step to identify Potentially Dangerous Glacial Lakes (PDGLs) and evaluating of hazards associated with them.

GLOF events have been widely reported throughout the Himalayas (Westoby et al. 2014b; Nie et al. 2018; Lützow et al. 2023; Shrestha et al. 2023). Various factors such

as glacier-lake interactions (i.e. lake area, expansion, the distance between lake-front and glacier terminus), dam characteristics (i.e. moraine width, height, slope), surrounding geomorphology of lakes (i.e. avalanche, rockfall), meteorological (i.e. cloudburst) and seismic conditions destabilize the glacial lakes in the alpine region and contribute towards triggering a GLOF (Westoby et al. 2014a; Fischer et al. 2021). Thus, it is important to identify and prioritize the individual PDGLs in the context of GLOF susceptibility and hazard assessment. This study focuses on the Chenab basin, Western Himalaya where studies have indicated accelerated glacier shrinkage (Das et al. 2023a) and rapid increase of glacial lakes due to warming (Kumar et al. 2017; Prakash and Nagarajan 2017; Ali et al. 2023; Das et al. 2023a).

The objectives for mapping and classification of glacial lakes vary as per the study such as inventory and change analysis (Aggarwal et al. 2017; Khadka et al. 2018; Wilson et al. 2018; Rinzin et al. 2021; Wood et al. 2021; Ahmed et al. 2022; Agarwal et al. 2023), outburst flood probability (Aggarwal et al. 2017; Prakash and Nagarajan 2017; Khadka et al. 2021; Ahmed et al. 2022), and modelling and forecasting of GLOF events (Worni et al. 2013; Westoby et al. 2014a; Nie et al. 2020; Allen et al. 2021; Majeed et al. 2021; Sattar et al. 2021, 2023; Rinzin et al. 2023; Gouli et al. 2023). Therefore, accurate classification and correct boundary delineation of glacial lakes are the most important and challenging tasks for any of the above studies. Satellite images with better spatial and temporal resolutions offer great potential for continuous monitoring of glacial lakes situated in high mountain areas where, field investigations are very laborious and time-consuming, owing to rugged and inaccessible environmental conditions (Ahmed et al. 2022). Precise identification and mapping of glacial lakes depends on the availability of high-resolution images and appropriate mapping techniques. Studies have extensively used medium-resolution (30 m) Landsat images for lake mapping and classification in the Himalayas (Supplementary Table S1). Moreover, various studies have been carried out to explore the efficiency of different mapping techniques ranging from manual to automatic for the identification of glacial lakes from satellite images (Supplementary Table S1).

Thus, in this direction, several studies have mapped and inventoried glacial lakes in the Himalayan region based on the interpretation of satellite remote sensing datasets at regional (ICIMOD 2011; Wang et al. 2020a) and basin scales (Allen et al. 2016; Aggarwal et al. 2017; Bhambri et al. 2018; Khadka et al. 2018; Rinzin et al. 2021; Ahmed et al. 2022). For example, Allen et al. (2016) prepared an inventory for Himachal Pradesh using Landsat data of 2013–214. Similarly, Bhambri et al. (2018) prepared an inventory of 958 glacial lakes (size $>0.0005\,km^2$) for Himachal Pradesh (areal coverage $9.6 \pm 0.3\,km^2$) using the Linear Imaging Self-Scanning Sensor-IV (LISS IV) data. Khadka et al. (2018) prepared a detailed inventory of 1541 glacial lakes in the Nepal Himalayas with an areal coverage of $80.95\,km^2$. In the Bhutan Himalaya, Rinzin et al. (2021) mapped 2574 lakes ($156.63 \pm 7.95\,km^2$) in 2020 using Sentinel 2 data. However, to the best of our knowledge, no studies have investigated the glacial lake inventory and spatio-temporal evolution in the Chenab basin. Few studies have been published on mapping and monitoring of glacial lake in the Chandrabhaga basin (Kumar et al. 2017; Prakash and Nagarajan 2017, 2018; Deswal et al. 2020; Kaushik et al. 2020; Kumar et al. 2021; Das et al. 2023a). Spatio-temporal evolution and

GLOF susceptibility of several glacial lakes have been studied such as Gepang Gath (Worni et al. 2013; Sattar et al. 2023), Samudra Tapu (Kumar et al. 2017; Kaushik et al. 2020), Panchi Nala (Das et al. 2023a), and Neelkanth lake (Deswal et al. 2020). Prakash and Nagarajan (2017) reported glacier spatio-temporal dynamics and GLOF susceptibility of 16 moraine-dammed lakes in the Chandrabhaga basin from 2000 to 2014 using Landsat data and the AHP method. In the adjacent Zanskar basin, studies have reported GLOF events and hazard assessment (Schmidt et al. 2020; Majeed et al. 2021). Here, for the first time, we mapped glacial lakes with improved spatial resolution (10 m) from Sentinel-2 data and presented GLOF susceptibility in the Chenab basin.

There are no straightforward quantitative techniques to identify and measure the GLOF potentiality of glacial lakes. Remote sensing-based hazard scores and vulnerability indices (ICIMOD 2011; Allen et al. 2016), empirical scoring system (Budhathoki et al. 2010), and intensity likelihood matrix (Bolch et al. 2008, 2011) have been used to estimate the GLOF susceptibility assessment. Multi-criteria based Analytical Hierarchical Process (AHP) has been widely employed to identify the PDGLs in the Swiss Alps (Huggel et al. 2004), British Columbia (McKillop and Clague 2007), Andes (Emmer and Vilímek 2013, 2014; Iribarren Anacona et al. 2014; Kougkoulos et al. 2018; Mergili et al. 2020), and in the Himalayan region (Bolch et al. 2011; Aggarwal et al. 2017; Khadka et al. 2021; Rinzin et al. 2021; Zhang et al. 2022). A variety of factors have been used to appraise the PDGLs across the Himalayas (Zhang et al. 2022) and Tibetan plateau (Allen et al. 2019). Studies have reported GLOF susceptibility of glacial lakes using multicriteria-based AHP techniques in the Western (Allen et al. 2016; Prakash and Nagarajan 2017), Central (Rounce et al. 2016; Khadka et al. 2021; Mal et al. 2021), and Eastern Himalayas (Aggarwal et al. 2017; Rinzin et al. 2021). In this context, the multi-criteria based AHP provides a first-hand opportunity to examine the GLOF susceptibility of glacial lakes, benefiting in early warning and disaster risk reduction of downstream communities.

Therefore, based on the preceding discussion, this study aims to identify and classify glacial lakes in the Chenab basin of the Western Himalayas using remote sensing techniques supported by extensive field validations. The study also analyzes the spatio-temporal changes in these lakes concerning their GLOF susceptibility. This study is divided into three parts. The first part focuses on mapping and generating a lake inventory and classification based on the morphological and topographical characteristics. The second part focuses on the spatio-temporal evolution and dynamics of lakes during the last three decades (1990–2022), and the last part focuses on the identification of GLOF susceptibility and hazard level.

2. Study area

The Chenab (also known as the Chandrabhaga River), a transboundary river, is one of the five main constituents of the Indus system (Figure 1A). Chandra and Bhaga Rivers constitute the upper catchment of the basin. Two rivers converge at Tandi in Himachal Pradesh to form the Chenab River, which then flows for 130 km before

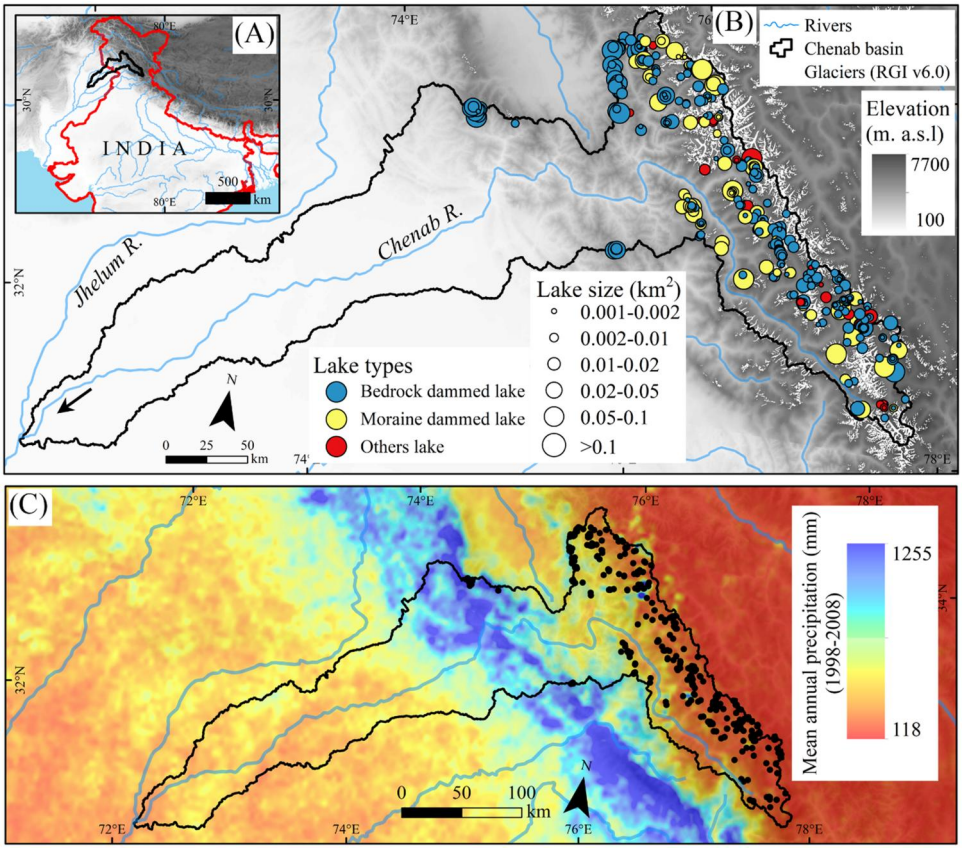

Figure 1. (A) Location of Chenab basin in Western Himalayas. (B) Distribution of glacial lakes (>0.001 km^2) in 2022. Elevation from GTOPO30 DEM is used in the background. The black arrow shows the river flow directions. No ice-dammed and landslide-dammed lakes were identified in the Chenab basin. (C) Distribution of lakes (black circles) under different precipitation regimes in Western Himalayas. Tropical Rainfall Measurement Mission (TRMM) precipitation map was obtained from Bookhagen and Burbank (2006).

entering Jammu and Kashmir (J&K) state, India. Then, Chenab flows through the Jammu region of J&K state into the plains of Punjab, Pakistan, before ultimately draining into the Indus River. The catchment of the Chenab is elongated in shape and covers an area of ~45,000 km^2 (Figure 1B). This region of the Himalayas comprises two NW-SE trending mountain ranges, the Pir-Panjal and Great Himalaya, which are separated by the major valley of the Chandra River. The upper part of the basin is located between the Zanskar and the Pir-Panjal ranges whereas the lower part is located in the Dhauladhar and the other outer ranges of the Himalayas. The topography of the basin is steep, and the glaciers are concentrated in the east. The elevation ranges from 350 to 7500 meters above sea level (m asl), and the westward terrain is lower than the eastward terrain. The majority of the large glaciers in the basin (i.e. Samudri Tapu, Bara Shigri, Miyar) are situated in the greater Himalayan range (Das et al. 2023b).

The climate of the region varies both altitudinally and geographically (Bookhagen and Burbank 2006), with a strong N–S precipitation gradient (Figure 1C). The

climatic conditions vary from hot and humid tropical in lower valleys to cool temperatures above ~1500–2000 m asl. As elevation increases, this climate gradually becomes colder, eventually transitioning to an extreme polar type at higher elevations (Padder et al. 2022). Chenab basin lies in the transition between the monsoon-dominated Pir-Panjal range in the south and the westerly-dominated Trans-Himalaya in the north. Seasonal distribution of precipitation is characterized by two major circulation systems: (1) mid-latitude westerlies in the winter months and, (2) south Asian monsoon in the summer months (Das et al. 2023b). Mean monthly precipitation reaches the maximum in June and July months and the minimum in November months. In the higher altitudes (>3500 m asl), more than 80% of precipitation occurs as snowfall (Das and Sharma 2019; Das et al. 2023b). Chenab River catchment is characterized by a dominance of snow, with ~65% of its precipitation occurring during the monsoon and pre-monsoon seasons. In contrast, winter contributes ~26% of the precipitation in the form of snow (Ali et al. 2021). As a result, the river experiences a substantial increase in flow due to intense monsoon precipitation, further amplified by the concurrent snowmelt during the summer season (Ali et al. 2021). The peak flow in the Chenab River catchment occurs between June and September. Distinct physiographical settings and climatic patterns make this basin ideal for studying the evolution and dynamics of glacial lakes in warming climatic scenarios.

The basin accommodates different litho-tectonic units of the Western Himalayas which range from Proterozoic to recent (Padder et al. 2022). In the upper reaches, the Chenab River cuts the higher Himalayan metamorphic, including haimantas, crystalline complex of the late Proterozoic age (Padder et al. 2022). Seismologically, this region falls under moderate to severe earthquake zones (Supplementary Figure S1). Several small to large (spanning from 30 to 1000 MW) hydroelectrical projects have been proposed to satisfy the regional energy needs (Supplementary Figure S2).

3. Data and methods

3.1. Remote sensing data

Freely available remotely sensed data ranging from medium to high resolution, Digital Elevation Models (DEMs) were used to examine the evolution and dynamics of glacial lakes in the Chenab basin (Table 1). Terrain-corrected Thematic Mapper (TM; 30 m) from Landsat 5, Enhanced TM+ (ETM+; 30 m) from Landsat 7, and Operational Land Imager (OLI; 30 m) from Landsat 8 images were used to digitize the lake outlines of 1990, 2000, and 2015, respectively. The latest lake outlines were mapped from the Sentinel 2 images of 2022 with 10 m spatial resolution. We used orthorectified images of 2013 from Resourcesat-2 LISS IV data (5 m) for lake mapping and validation for the part of the upper Chandrabhaga basin (Das et al. 2023a). All images were acquired for the post-ablation period (September–November) to minimize the seasonal snow cover effect. Details of scenes used from different sensors are provided in Supplementary Table S2. In addition, high-resolution imagery (<1 m) from Google Earth (GE), the Advanced Spaceborne Thermal Emission and Reflection Radiometer (ASTER), and High Mountain Asia (HMA) DEMs were used to obtain

Table 1. Data sources.

Date of acquisition	Satellite sensors	Spatial resolution (m)	Spectral bands	Source	Applications	Methods
Satellite remote sensing data						
1990	Landsat 5 (TM)	30	visible; mid-infrared	USGS	Change analysis	NDWI + Manual mapping
2000	Landsat 7 (ETM+)	15, 30	Panchromatic; visible; mid-infrared	USGS	Change analysis	NDWI + Manual mapping
2015	Landsat 8 (OLI)	15, 30	Panchromatic; visible; mid-infrared	USGS	Change analysis	NDWI + Manual mapping
September 10-20, 2022	Sentinel 2B (MSI)	10	visible; mid-infrared	COAH	Inventory, change analysis	NDWI + Manual mapping
2014–2022	Google Earth	< 1	True color single band with 3D capabilities	GE software	Lake area mapping, dam characteristics, geomorphology	Manual mapping
	ASTER GDEM	30 m		Earth data	Topographic analysis	
DEMs	HMA DEM	8 m		NSIDC	Dam characteristics, geomorphology	

Details of scene ID and number of images used for the present study is provided in supplementary information. USGS: United States Geological Survey; COAH: Copernicus Open Access Hub; NSIDC: National Snow and Ice Data Center; GE: Google Earth; TM: Thematic Mapper, ETM+: Enhanced Thematic Mapper Plus; OLI: Operational Land Imager; MSI: Multi-Spectral Scanner; ASTER: Advanced Spaceborne Thermal Emission and Reflection Radiometer; HMA: High Mountain Asia; NDWI: Normalized Difference Water Index.

information about topographic parameters and dam characteristics. Geological and seismic maps were obtained from Padder et al. (2022).

3.2. Lake mapping and classification

The manual delineation of the boundaries of each single lake is preferred to an automatic procedure. Even though automatic lake identification procedures from optical or radar satellite imageries are well established (cf. Huggel et al. 2002; Strozzi et al. 2012; Wangchuk and Bolch 2020), it has been found that, in specific cases, the requirement of a substantial amount of manual post-processing outweighs the advantages of automated lake detection. Factors such as mountain shadows, cloud cover, and seasonal snow introduce significant errors (Zhang et al. 2015; Shukla et al. 2018). Consequently, manual post-editing is almost imperative and is recommended in nearly all automated lake mapping methods (Mergili et al. 2013; Wood et al. 2021). Here, on-screen digitization techniques of glacial lakes comprise of firstly, highlighting water bodies using the Normalized Difference Water Index ($NDWI = B_{NIR} - B_{GREEN}/B_{NIR} + B_{GREEN}$) from Sentinel-2 imageries (Figure 2), followed by overlaying of NDWI image on standard False Color Composite (FCC: bands: 8-4-3). No threshold was applied to NDWI images (Figure 2). Later, all extracted lake boundaries were exported to GE for further checking and correction using high-resolution 3-D images

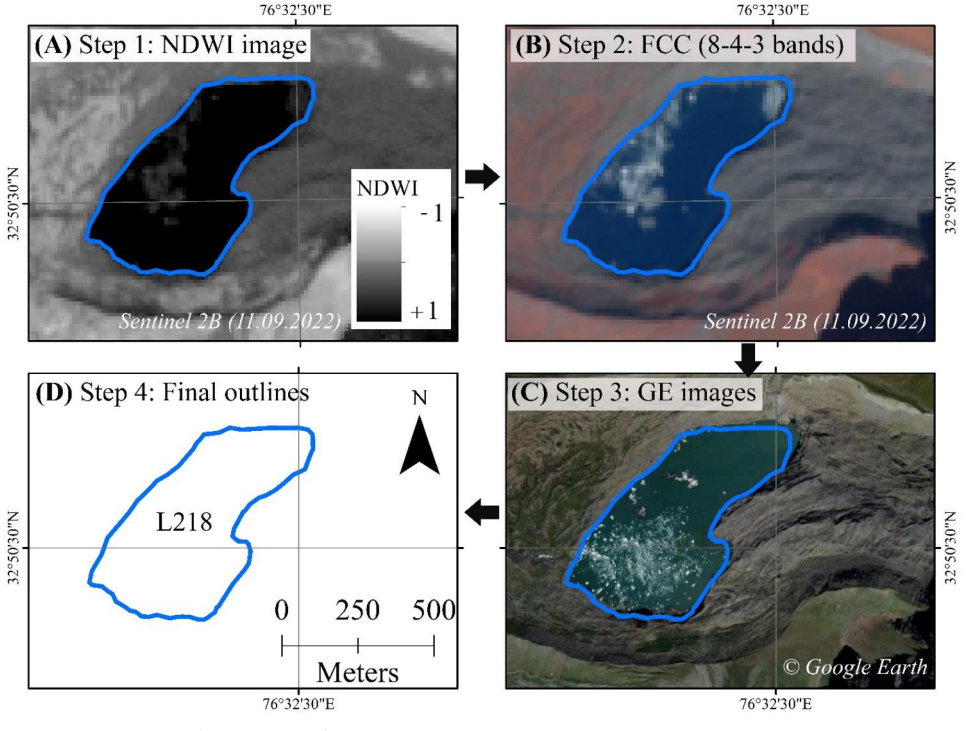

Figure 2. Example of mapping of glacial lakes. (A) Lake boundary was manually digitized using an NDWI image. (B) Lake outlines were overlaid on standard FCC and checked. (C) Lake outlines were further manually checked and corrected using high-resolution google earth images. (D) Final lake boundary. L218 is the lake id for Kadu Nala lake.

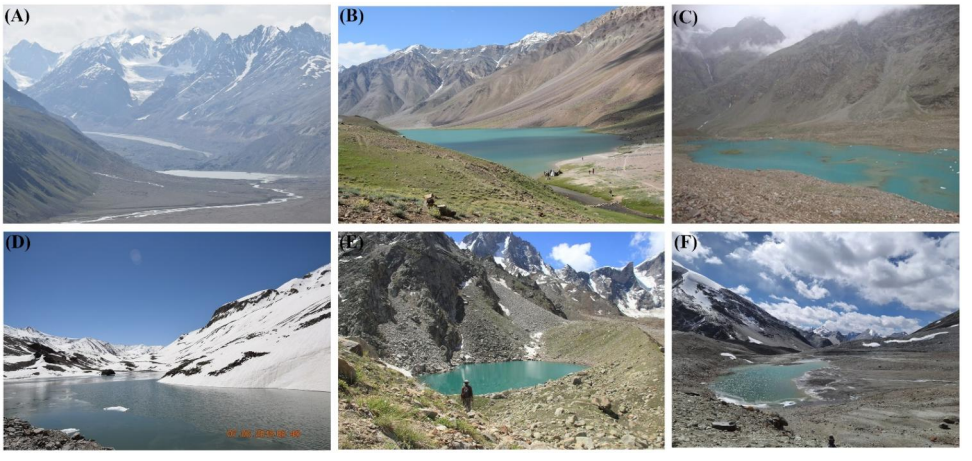

Figure 3. Field photographs of few pro-glacial lakes from the Chenab basin. (A) a typical pro-glacial moraine-dammed Samudri Tapu lake. (B) a bedrock-dammed Chandra Tal. (C) Moraine-dammed Gepan Gath lake. (D) Bedrock-dammed Suraj Tal. (E) Moraine-dammed Neelkanth lake. (F) Bedrock-dammed Shingo La lake.

(Figure 2C). Previous studies consistently utilized a 10 km buffer area from the nearest glacier to identify glacial lakes (Gardelle et al. 2011; Zhang et al. 2015; Nie et al. 2017; Khadka et al. 2018; Shukla et al. 2018). In this study, a preliminary step involved creating a 10 km buffer area from the closest glacier termini using Randolph Glacier Inventory (RGI) outlines obtained from Global Land Ice Measurements from Space version 7 (GLIMS v7), and the lowest elevation of the glacial lake was recorded at ~3390 m asl. This recorded elevation served as the minimum threshold and a comprehensive assessment was conducted to detect the presence of glacial lakes. This method ensured the inclusion of the maximum number of glacial lakes in the analysis. All lakes $<0.001\,km^2$ were removed because their change detection was regarded as too uncertain given the spatial resolution (10 m) of Sentinel 2 images (Gardelle et al. 2011; Zhang et al. 2015). The lake outlines digitized from the remote sensing data were extensively validated based on the field observation during 2010–2022 (Figure 3).

First, all the mapped lakes were classified into broad two groups followed by Zhang et al. (2015): non-glacier-fed and glacier-fed (Figure 4). We followed the classification scheme of Carrivick and Tweed (2013) and Aggarwal et al. (2017) for the categorization of glacial lakes based on their geomorphology, and the lakes were grouped into five main classes: bedrock-dammed lakes (BDL), moraine-dammed lakes (MDL), ice-dammed lakes (IDL), landslide-dammed lakes (LDL), and other lakes (OL).

3.3. Inventory and temporal changes

An inventory of glacial lakes was generated for the year 2022 using Sentinel 2 (10 m) images. Studies have reported that higher spatial resolution of Sentinel 2 images reduces the uncertainty of lake outline delineation, compared to the 30 m Landsat images (Aggarwal et al. 2017; Rinzin et al. 2021). Followed by Aggarwal et al. (2017) and Rinzin et al. (2021), lakes identified and mapped in section 3.2 were further

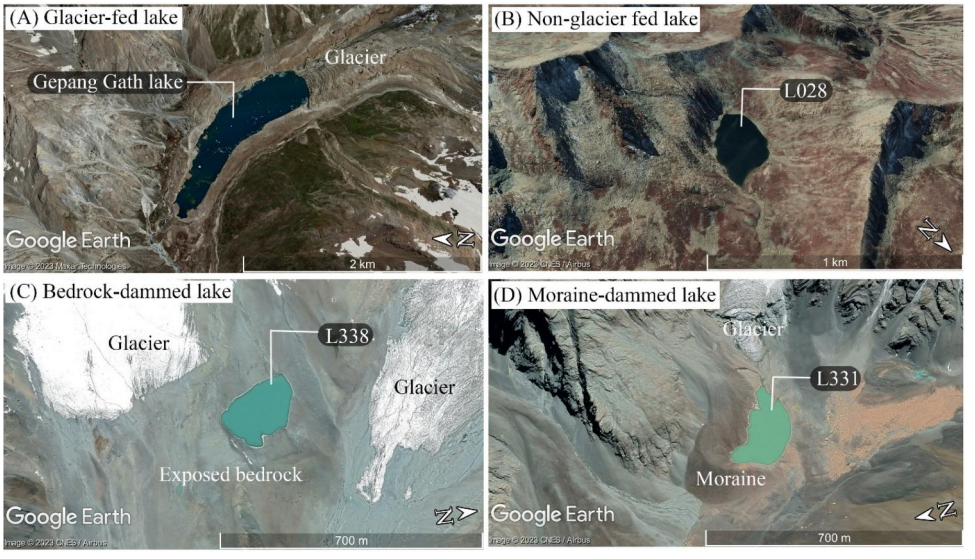

Figure 4. Typical examples of different lake types. (A) Glacier-fed lake. (B) Non-glacier fed lake. (C) Bedrock-dammed lake. (D) Moraine-dammed lake.

described by several quantitative and qualitative parameters. Each lake was assigned a unique label. Quantitative parameters (i.e. area, perimeter, elevation) were derived automatically from satellite images and ASTER DEMs in GIS environment. Glacial lake volume was estimated using the following empirical formula from Huggel et al. (2004):

$$V = 0.104 \times A^{1.42} \tag{1}$$

Where V is volume and A is the surface area of the lake. Although Huggel et al. (2004) performed empirical calculations based on the data from the Swiss Alps, studies have successfully used this formula for estimating lake volume in the Himalayas (ICIMOD 2011; Aggarwal et al. 2017; Khadka et al. 2018; Rinzin et al. 2021). Qualitative parameters (i.e. lake type) were manually assigned to each lake by visual interpretation (Supplementary Table S3).

Temporal changes were calculated for lakes $>0.05\,km^2$ in size, as smaller lakes are difficult to precisely map from medium resolution (30 m) Landsat images (Rinzin et al. 2021). Glacial lake ($\geq 0.05\,km^2$) outlines of 2022 were overlaid on multitemporal satellite images (1990, 2000, and 2015) and manually digitized. We performed multitemporal change detection for different types of glacial lakes for four distinct time spans: 1990–2000, 2000–2015, 2015–2022, and 1990–2022.

3.4. GLOF susceptibility assessment

3.4.1. Factor selection

We designed and applied the Multi-Criteria Decision Making (MCDM) based AHP method to ascertain the GLOF susceptibility. We complied several GLOF susceptibility factors from previous studies in the Himalayan region (ICIMOD 2011; Emmer

and Cochachin 2013; Emmer and Vilímek 2014; Emmer et al. 2016; Aggarwal et al. 2017; Prakash and Nagarajan 2017; Khadka et al. 2021; Rinzin et al. 2021; Fischer et al. 2021; Zhang et al. 2022; Table 2 and references therein). Various factors can initiate GLOF events from moraine-dammed lakes either by dam overtopping or failure (Emmer and Vilímek 2014; Westoby et al. 2014a). Factors used in previous work on GLOF susceptibility and hazard assessment can be broadly categorized into four groups: (i) lake-glacier characteristics, (ii) dam characteristics, (iii) lake surroundings morphology, and (iv) other factors (Emmer and Vilímek 2014; Worni et al. 2014; Allen et al. 2019; Mal et al. 2021; Fischer et al. 2021; Zhang et al. 2022). A flowchart of methodology adopted for GLOF susceptibility is presented in Figure 5.

I. We used glacier lake area (F1), expansion rate (F2), distance between lake-front and parent glacier terminus (F3), and slope between lake and glacier tongue (F4) as significant factors of outburst probability (Figure 6). According to Nagai et al. (2017), a glacial lake size of 0.01 km^2 is deemed sufficiently large to pose a significant hazard to downstream settlements. For regional hazard assessment, >0.1 km^2 area threshold is commonly used (Allen et al. 2019), while Nie et al. (2018) suggested a minimum area threshold of 0.05 km^2 based on 51 past GLOF events in the Himalayan region. Previous studies have estimated the GLOF hazard assessments of glacial lakes >0.1 km^2 in size in the Western (Worni et al. 2013), Central (Rounce et al. 2017) Himalayas, and in the Tibetan plateau (Allen et al. 2019). In the Bhutan Himalaya, among 13 lakes with a GLOF history, 10 have areas ranging from 0.01 to 0.06 km^2 (Nagai et al. 2017). Recent GLOF events in the Indian (Das et al. 2015) and Nepalese Himalayas (Nie et al. 2018) have been reported from glacial lakes <0.1 km^2 in size. Lakes with larger surface area are more prone to impact from mass movement from the surrounding terrain, thus may cause higher damage downstream (Bolch et al., 2008; Prakash and Nagarajan, 2017). In this study, glacial lakes with an area of ≥0.05 km^2 were considered in the GLOF susceptibility assessment as suggested by other studies in the Himalayas (ICIMOD 2011; Nie et al. 2018; Veh et al. 2020; Khadka et al. 2021). We assumed that the magnitude of GLOF increases with the area of the lake, so we categorized them as low risk for lakes <0.06 km^2, medium risk for lakes ranging 0.06–0.1 km^2, and high risk for lakes >0.1 km^2. The lake expansion rate (F2) was calculated from multitemporal satellite images. We divided the expansion rate into three groups: >100% (high), 50–100% (moderate), and <50% (low) during the last 30 years (Aggarwal et al. 2017; Prakash and Nagarajan 2017). Glacier-lake proximity (F3) significantly influences the lake dynamics (Huggel et al. 2004; Worni et al. 2013; Westoby et al. 2014a; Cook et al. 2016; Fan et al. 2019; Wang et al. 2020b; Hu et al. 2022). A lake in contact with a glacier may experience faster growth due to the continuous glacier retreat and is more susceptible to GLOF due to the ice calving on the lake, which can generate an outburst due to the overtopping of lake water (Carrivick and Tweed 2013). Distance between the glacier terminus and the lake-front was measured using GE (Figure 6) and categorized into three classes: lakes in contact with the glacier (high), <500 m (moderate), and >500 m (low). The slope between the

Table 2. Index values of factors with sub-criteria for GLOF susceptibility assessment adapted and modified from previous studies.

Factors ID	Factors name	Definition of factors	Methods of extraction	Class/alternatives	Probability of outburst	Index values	References
F1	Lake area	Surface area digitized from remote sensing images	Manually digitized from the satellite images	>0.1 km^2 0.06-0.1 km^2 < 0.06 km^2	High Medium Low	1 0.5 0.25	1, 2, 4, 5, 7, 8, 11, 12, 14, 15, 16, 19, 22, 24, 28, 30, 31, 32, 33, 37, 38, 39, 40, 41, 42, 45, 47, 48, 49, 50, 51
F2	Expansion rate	Expansion rate of lakes during the observation period in percentage	Manual digitized from multitemporal images	>100% 50-100% <50%	High Medium Low	1 0.5 0.25	2, 5, 7, 8, 11, 13, 14, 15, 19, 21, 22, 23, 24, 25, 26, 27, 31, 32, 33, 34, 39, 45, 47, 48, 49, 51, 52
F3	Glacier-lake distance	Horizontal distance between the lake and its parent glacier (in meter)	Manually measures in GIS environment, Google Earth	In contact < 500 m > 500 m	High Medium Low	1 0.5 0.25	2, 3, 4, 5, 6, 7, 8, 9, 11, 13, 14, 15, 16, 19, 24, 27, 34, 35, 37, 38, 39, 40, 41, 42, 45, 47, 48, 49, 50, 51, 52
F4	Slope between lake and glacier	Slope between the lake and its parent glacier (in degree)	Manually measured from elevation profile	> 21 ° 12-21 ° < 12 °	High Medium Low	1 0.5 0.25	3, 14, 34, 38, 39, 42, 47, 48, 49, 50, 52
F5	Moraine width & height ratio	Ratio between dam height and width	Manually measured from elevation profile	< 0.1 0.1-0.5 > 0.5	High Medium Low	1 0.5 0.25	9, 13, 14, 18, 20, 29, 39, 42, 44, 45, 49, 50, 52
F6	Freeboard	Height difference between lake water and crest of dam	Manually measured from DEM and Google Earth	0 (surface drainage) < 5 m > 5 m	High Medium Low	1 0.5 0.25	6, 13, 14, 15, 18, 20, 25, 28, 29, 31, 33, 35, 38, 42, 44, 45
F7	Dam distal-face slope	Slope of moraine frontal region	Manually measured from DEMs	>20 ° 12-20 ° <12 °	High Medium Low	1 0.5 0.25	1, 3, 10, 11, 13, 15, 18, 20, 21, 23, 39, 41, 42, 50
F8	Mass movement probability	Rock fall and avalanche probability	Modelled and measured using DEMs, topographic potential area	>1 km^2 0.5 – 1 km^2 <0.5 km^2	High Medium Low	1 0.5 0.25	1, 9, 10, 11, 13, 17, 18, 19, 20, 21, 23, 24, 25, 28, 29, 30, 31, 36, 39, 40, 41, 42, 43, 44, 45, 46, 47, 48, 49, 51, 52
F9	Cloudburst probability	a sudden, very heavy rainfall, usually local in nature and of brief duration	Literature assessment	Frequent Sporadic Unlikely	High Medium Low	1 0.5 0.25	14, 35, 39, 44, 46
F10	Seismicity	the occurrence or frequency of earthquakes in a region.	Seismic zone classification	Zone 5 (PGA> 0.5 g) Zone 4 (PGA 0.5–0.35 g) Zone 3 (PGA 0.35–0.15)	High Medium Low	1 0.5 0.2.5	14, 15, 16, 32, 33, 35, 39

PGA = peak ground acceleration, a parameter to measure earthquake intensity. Reference sources: 1: Allen et al. (2019); 2: Wang et al. (2020); 3: Wang et al. (2011); 4: Fan et al. (2019); 5: Wang et al. (2015); 6: Liu et al. (2020); 7: Khanal et al. (2015); 8: Wang et al. (2012); 9: Wang et al. (2008); 10: Dubey and Goyal (2020); 11: Khadka et al. (2021); 12: Ali et al. (2023); 13: Prakash and Nagarajan (2018); 14: Prakash and Nagarajan (2017); 15: Aggarwal et al. (2017); 16: Jha and Khare (2017); 17: Allen et al. (2016); 18: Worni et al. (2013); 19: Aggarwal et al. (2016); 20: Deswal et al. (2020); 21: Rounce et al. (2017); 22: Begam and Sen (2019); 23: Rounce et al. (2016); 24: Khanal et al. (2015); 25: Bolch et al. (2008); 26: Nagai et al. (2017); 27: Falatkova et al. (2019); 28: Petrakov et al. (2020); 29: Petrov et al. (2017); 30: Kapitsa et al. (2017); 31: Bolch et al. (2011); 32: Gruber and Mergili (2013); 33: Mergili et al. (2011); 34: Drenkhan et al. (2019); 35: Kougkoulos et al. (2018); 36: Frey et al. (2018); 37: Emmer et al. (2016); 38: Emmer and Vilímek (2014); 39: Emmer and Vilímek (2013); 40: Cook et al. (2016); 41: Iribarren Anacona et al. (2014); 42: McKillop and Clague (2007); 43: Clague and Evans (2000); 44: Huggel et al. (2004); 45: Huggel et al. (2002); 46: Zhang et al. (2022); 47: Rinzin et al. (2021); 48: Islam and Patel (2020); 49: Zhang et al. (2023); 50: Hu et al. (2022); 51: Rawat et al. (2023); 52: Ahmed et al. (2022).

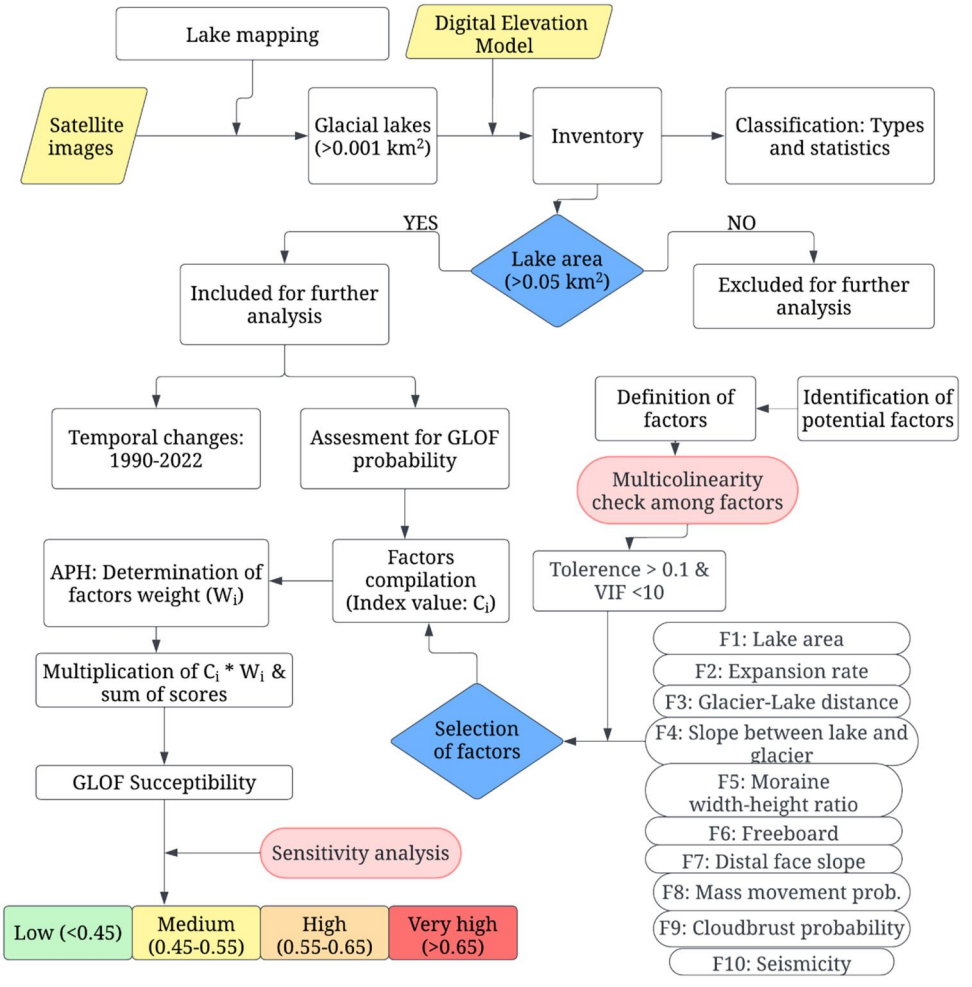

Figure 5. Flowchart of methodology.

lake and the terminus of parent glacier (F4) is another key factor that influences ice avalanches and future lake growth (Emmer and Vilímek 2013; Emmer et al. 2016; Drenkhan et al. 2019; Allen et al. 2021; Khadka et al. 2021). We calculated the slope by dividing the height difference between the lake and the glacier terminus by the distance (Figure 6). The slope between the lake and glacier terminus was categorized into three classes/alternatives (>21°: high; 12–21°: medium; <12°: low) to assign index values (Table 2).

II. The probability of failure of a moraine-dammed lake depends on dam geometry (dam width, height, moraine distal face slope), dam material properties (weight, cohesion, porosity, grain size distribution, etc.), and freeboard of the lake (Worni et al. 2013; Emmer and Vilímek 2014; Worni et al. 2014; Allen et al. 2019). We used moraine width and height ratio (F5), freeboard (F6), and distal slope of moraine crest (F7) as significant factors for outburst susceptibility assessment (McKillop and Clague 2007; Bolch et al. 2011; ICIMOD 2011; Mergili et al. 2011; Aggarwal et al. 2017; Prakash and Nagarajan 2017; Khadka

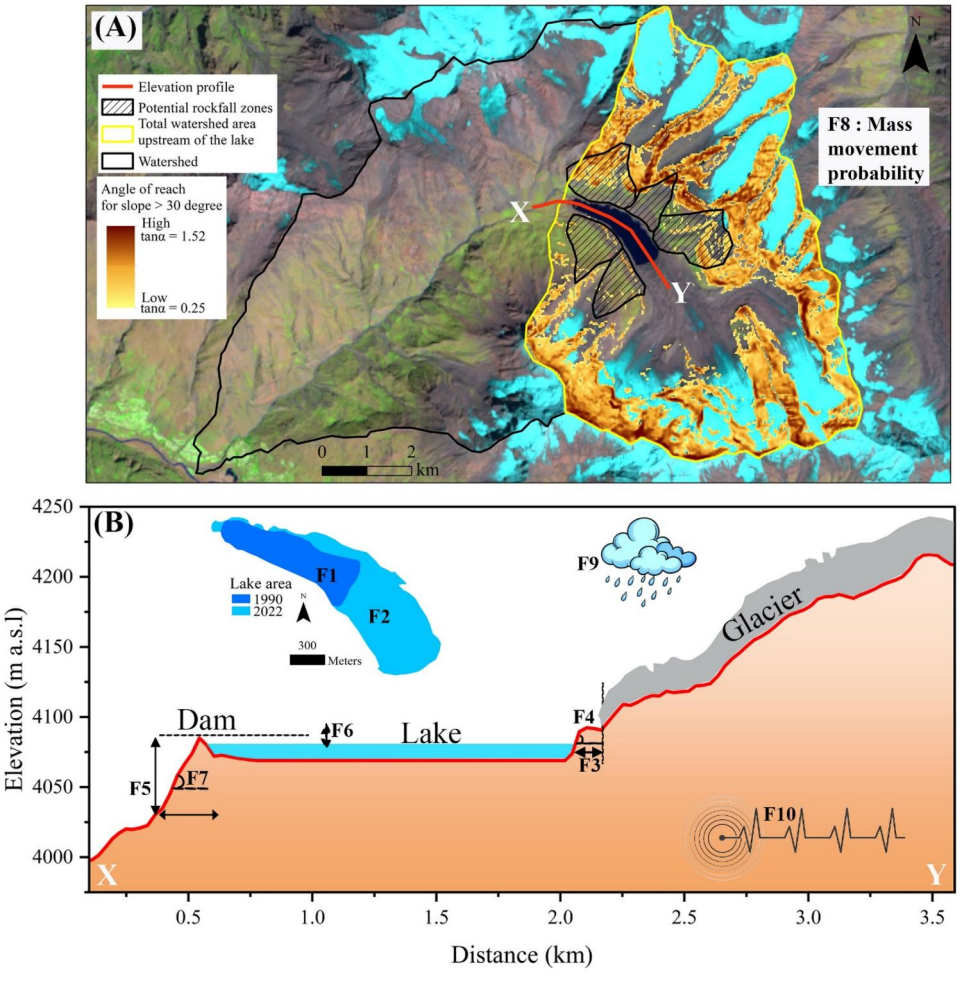

Figure 6. Factors for outburst susceptibility assessed in this study. (A) Modelled mass movement probability of Gepang Gath lake. (B) A schematic diagram of different factors assessed and measured along XY elevation profile. (F1) lake area; (F2) increase in lake area; (F3) lake–glacier proximity (horizontal distance); (F4) slope between lake and glacier; (F5) moraine width-to-height ratio; (F6) freeboard; (F7) slope of distal face of moraine; (F8) mass movement probability; (F9) cloudburst or extreme rainfall event; and (F10) seismicity. The background is false color composite (bands: 7-5-4) of Landsat 8 image. Elevation profile was drawn from ASTER DEM.

et al. 2021; Rinzin et al. 2021; Ahmed et al. 2022) as reported in the other studies in the Himalayas (Table 2). The dam width-to-height ratio influences the hydraulic pressure, leading to piping within the moraine dam and subsequent slope failure of the moraine (Worni et al. 2014; Majeed et al. 2021). The slope of the distal face of moraine exhibits the stability and erodibility, which may lead to dam failure (Westoby et al. 2014a). The vertical distance between the lake water level and the moraine crest is known as the freeboard which exhibits the potential of topping of water due to sudden mass movement into the lake (Emmer and Vilímek 2013). Here, we used 30 m ASTER DEM for the extraction of dam characteristics for each lake. Previous studies have used ASTER DEM

for generating dam-related parameters for GLOF susceptibility assessment in Bhutan (Rinzin et al. 2021), Sikkim (Aggarwal et al. 2017), Nepal (Khadka et al. 2021), and Western Himalaya (Prakash and Nagarajan 2017; Ahmed et al. 2022). In addition to this, HMA DEM (8 m) was used based on availability. Dam characteristics were extracted from DEMs and 3D GE imageries using elevation profiles (Figure 6; Supplementary Figures S3 and S4). We measured the dam width-to-height ratio and assigned index values as: <0.1 (high), 0.1–0.5 (medium), and >0.5 (low). We assigned high index values for lakes having surface drainage (i.e. zero freeboard), followed by <5 m as a medium, and >5 m as low values (Table 2; Prakash and Nagarajan 2017). High index value was assigned to dams having a frontal slope of $>20°$, followed by 12–20° as medium, and $<12°$ as low values (Wang et al. 2011).

III. Mass movement (rockfall, ice avalanche) of the lake's surrounding area is an important outburst-triggering factor (Worni et al. 2014; Prakash and Nagarajan 2017; Rinzin et al. 2021). We considered ice or rock avalanches to represent mass movement (F8) combinedly. Avalanche is the major outburst-triggering factor in the Himalayas (Nie et al. 2018; Allen et al. 2019; Zhang et al. 2022). Thus, the mass movement factor was ranked as the highest priority by expert judgment, and the maximum weight assigned to this factor from AHP is justifiable. Here, following Allen et al. (2019), we modelled the ice or rock avalanche probability zones (i.e. topographic potential area). First, we demarcated the total watershed area upstream of the lake using a hydrology tool in ArcGIS software (Figure 6A). Later, within each lake watershed, the potential topographic area was calculated for all grid cells fulfilling (1) slope $>30°$ and (2) trajectory slope of 17° ($\tan\alpha = 0.25$). This approach assigns greater significance to steep slopes that are nearer to a lake, as these slopes are more likely to generate avalanches that can reach the lake. In addition, lakes located in large watersheds where potential avalanche-prone valley walls are located at a horizontal distance of >2 km were excluded, assuming that the avalanche or mass movement does not hit the lake directly (Khadka et al. 2021). A topographic potential area of $>1\,km^2$ was assigned as a high index value, 0.5–1 km^2 as medium value, and $<0.5\,km^2$ as a low value (Table 2; Supplementary Table S11).

IV. We used cloudbursts as meteorological events and earthquakes as seismic events that can trigger GLOF events (Das et al. 2015; Nie et al. 2018; Zhang et al. 2022). A sudden cloudburst may rapidly increase the water level in the lake, thus increasing hydrostatic pressure, resulting in the failure of the dam and outburst (Worni et al. 2014). The probability of extreme rainfall or cloudburst in the study area is 1 in 12 years and is categorized as a low-risk area (Prakash and Nagarajan 2017). A strong earthquake can trigger mass movement into the lake, which can generate a displacement wave. Further, blockade of the dam outflow path from mass movement can lead to dam overflow and eventually to dam failure (Emmer and Vilímek 2013; Worni et al. 2014). Several GLOF events were reported to have been triggered by an ice/rock avalanche or landslide, initiated by a high-magnitude earthquake in the central Himalayan region (Ives et al. 2010; Osti et al. 2011; Byers et al. 2019). However, based on empirical evidence,

a recent study (Wood et al. 2024) suggests that earthquake rarely triggers GLOFs in the tropical Andes. The study area falls within moderate to high seismic zones (Supplementary Figure S1), having Peak Ground Acceleration (PGA) values between 0.35 and 0.5 g (Prakash and Nagarajan 2017). We overlaid glacial lake outlines on seismic maps, and assigned index values: high (zone V), medium (zone IV), and low (zone III).

3.4.2. Weight assignment and GLOF susceptibility index

We used the MCDM based AHP method to assign the weight of each GLOF susceptibility factor. The AHP is a semi-quantitative decision-making technique using weights through pairwise comparison among different factors without inconsistencies (Satty 1990). Several studies have used the AHP method for GLOF susceptibility assessment of glacial lakes in the Himalayan region (Aggarwal et al. 2017; Prakash and Nagarajan 2017; Khadka et al. 2021; Zhang et al. 2022).

For determining the susceptibility of individual lakes to possible GLOF events in the future, weights were assigned to each parameter (Table 3). Such weights were assigned mainly by the authors'/users' expertise and know-how, along with their understanding of the interaction/impact of these different parameters for possible GLOF events for individual lakes, as reported in previous studies (Supplementary Table S5–S12). The AHP technique succinctly summarises the authors' perceptions and judgments into a multi-level hierarchical configuration following their significance. It simplifies the complex assemblage of connections among the different parameters through the comparison matrix and reduces biases through the analysis's consistency. To find out the relative significance of the parameters, a pairwise comparison matrix was computed (using the degree of importance scale ranging from 1 to 9, i.e. 1 denotes equal importance and 9 denotes extreme importance of one parameter concerning the other) and normalized to determine the weights and ranks of each parameter (see Supplementary Tables S5–S12). The final weights for each parameter were calculated by multiplying the factor weights from the AHP with the class index following the given formula:

$$GLOF\ \ index = \sum_{i=0}^{n} F_w * C_i \tag{2}$$

where F_w is the factor weights and C_i is the class index value. The susceptibility values obtained from the above equation range from 0.25 to 0.72 and are thereby classified into four classes: very high (>0.65), high (0.65–0.55), medium (0.55–0.45) and low (<0.45), as reported in the region (Prakash and Nagarajan 2017).

3.5. Mapping uncertainty and sensitivity analysis

3.5.1. Lake mapping uncertainty

The lake area uncertainty (δ) is calculated using the following equation (Hanshaw and Bookhagen 2014; Zheng et al. 2021):

$$\delta = \frac{P}{G} \times \frac{G^2}{2} \times 0.6872 \tag{3}$$

Table 3. Pairwise comparison matrix and weight of factors computed using the AHP factors.

Factors ID	Factors title	F8	F5	F6	F1	F2	F7	F3	F4	F9	F10	CW	Rank	Tolerance	VIF
F8	Mass movement probability	1	2	3	4	5	6	7	8	9	10	0.29	1	0.67	1.49
F5	Moraine width & height ratio	0.50	1	2	3	4	5	6	7	8	9	0.21	2	0.55	1.81
F6	Freeboard	0.33	0.50	1	2	3	4	5	6	7	8	0.15	3	0.45	2.20
F1	Lake area	0.25	0.33	0.50	1	2	3	4	5	6	7	0.11	4	0.81	1.23
F2	Lake expansion rate	0.20	0.25	0.33	0.50	1	2	3	4	5	6	0.08	5	0.51	1.98
F7	Distal face slope	0.16	0.20	0.25	0.33	0.50	1	2	3	4	5	0.06	6	0.85	1.18
F3	Glacier-lake distance	0.14	0.16	0.20	0.25	0.33	0.50	1	2	3	4	0.04	7	0.25	4.08
F4	Slope between glacier and lake	0.13	0.14	0.16	0.20	0.25	0.33	0.50	1	2	3	0.03	8	0.31	3.20
F9	Cloudburst events probability	0.11	0.13	0.14	0.16	0.20	0.25	0.33	0.50	1	2	0.02	9	0.00	0.00
F10	Seismic zone	0.10	0.11	0.13	0.14	0.16	0.20	0.25	0.33	0.50	1	0.02	10	0.70	1.43

Tolerance and variance inflation factor (VIF) represent multicollinearity results of each factor. Factors are arranged based on ranks. CW = Criteria Weight.

where P is the perimeter of the glacial lakes, and G is the spatial resolution of the images used. The relative change in lake area between 1990 and 2022 and its uncertainties were estimated using the following equations (Zheng et al. 2021):

$$R = \frac{A_2 - A_1}{A_1} * 100\% \tag{4}$$

$$\delta R = \sqrt{\left(\frac{\delta A}{A_2 - A_1}\right)^2 + \left(\frac{\delta A_1}{A_1}\right)^2} \times R \tag{5}$$

$$\delta A = \sqrt{\delta A_1^2 + \delta A_2^2} \tag{6}$$

where R is the relative change in the glacial lake area and δR is its uncertainty; A_1, A_2 are the lake areas at the beginning and end of the period; δA_1, δA_2 are their uncertainties, respectively; and δA is total uncertainty.

3.5.2. AHP sensitivity analysis

The sources of uncertainties in the GLOF susceptibility assessment could arise from the satellite data used for preparing the inventory and the DEMs used for estimating the factors (Prakash and Nagarajan 2017; Khadka et al. 2021; Rinzin et al. 2021). The uncertainty of lake mapping affects the input values for lake area and expansion rate; however previous studies have successfully used a similar dataset (i.e. Sentinel-2) for preparing the inventory and computing the factors for the GLOF hazard and risk assessment in other parts of Himalaya (Rinzin et al. 2021). We performed an accuracy assessment for factors selection and outburst susceptibility using: (1) collinearity and consistency ratio check of AHP (Das et al. 2022), and (2) sensitivity analysis by shifting the class/alternative and modifying the GLOF susceptibility class (Khadka et al. 2021).

We performed a multicollinearity analysis to check the correlation among factors. The MCDM model encounters a significant statistical challenge known as multicollinearity, where one or more input factors, either dependent or independent variables–exhibit high correlation with each other or with a combination of other input factors. This phenomenon can substantially influence the model output due to the presence of linear relationships among the input factors (Shrestha 2020). Multicollinearity typically manifests when tolerance values fall <0.10 or the Variance Inflation Factor (VIF) >10 (Das et al. 2022). In such cases, it becomes necessary to eliminate these parameters from the analysis to mitigate the distortions caused by multicollinearity. Tolerance (T_i) and VIF (VIF_j) of any variables are calculated as follows:

$$T_i = 1\text{–}R_i^2 \tag{7}$$

$$VIF_j = \frac{1}{T_i} \tag{8}$$

These equations are applied iteratively across each input factor. After collecting data for each factor, the analysis was conducted using SPSS (v27.0.1) software. The results obtained for each factor (Table 3) indicate VIF and tolerance values of <10 and >0.1 respectively, at significance levels of $\rho < 0.01$ and $\rho < 0.05$. Consequently, there was no evidence of collinearity among the 10 factors, ensuring that the model results remained unaffected by multicollinearity issues.

The Consistency Ratio (CR) was utilized to guarantee the validity of the overall impact of various models utilized in AHP and expressed as:

$$CR = CI/RI \tag{9}$$

where CI is the consistency index and RI represents the random index of the hierarchical order of the matrix (Supplementary Tables S5–S12). The equation of CI is:

$$\frac{(\lambda_{\max} - n)}{(n-1)} \tag{10}$$

Where $\lambda_{\max}$ is the rule or most elevated eigenvector of the network and n demonstrates the number of select parameters. The CR value should be <0.1 to yield a significant outcome to continue with further analysis. The speed of productivity through CR can be decreased by auditing the decisions, as required. We obtained CR as follows:

$$\begin{aligned} \lambda_{\max} &= 10.54, \\ n &= 10, \\ CI &= \frac{(10.5464 - 10)}{(10-1)} = 0.0607, \\ RI &= 1.48, \\ CR &= \frac{0.0607}{1.48} = 0.0410, \\ Consistancy\ \ check &= 4.11\%. \end{aligned} \tag{11}$$

The overall consistency ratio was calculated as ~4%, which shows the high confidence in the correlation matrix among variables (Supplementary Tables S5–S12).

In a multi-criteria decision-based GLOF hazard assessment, sensitivity analysis (SA) plays a key role in determining how much uncertainty of the results of the assessment is influenced by the uncertainty of its input criteria. The validation of hazard assessment methods using past GLOF events has commonly been done in previous studies (Nie et al. 2018), to get a sectoral overview of the region. However, historical GLOF records are absent for the Western Himalayan region, which hinders validation against past events (Supplementary Figure S6). We followed the approach of Khadka et al. (2021) for SA. First, we checked the sensitivity of GLOF assessment by shifting the low and medium class/alternatives of F1 to medium and high classes, respectively keeping other factors constant. Similarly, SA was performed for the remaining nine factors (F2-F10). Later, SA was performed to check the extent to

which GLOF susceptibility of lakes will change when the susceptibility class is modified by ±5%, i.e. ±0.05 (Supplementary Tables S13 and S14).

4. Results

4.1. Inventory of glacial Lakes

In 2022, a total of 419 glacial lakes (>0.001 km^2) were mapped, covering a total area of 9.97 ± 0.69 km^2, heterogeneously distributed across the Chenab basin. A total of 225 lakes are identified as glacier-fed, comprising an area of 6.02 ± 0.37 km^2 (60% of total area). In contrast, non-glacier-fed lakes comprise an area of 3.95 ± 0.32 km^2 (Figure 7A). Among the lakes, 306 (4.21 ± 0.42 km^2) are bedrock-dammed, 80 (5.41 ± 0.23 km^2) are moraine-dammed, and 33 (0.35 ± 0.04 km^2) are other lakes. No ice-dammed and landslide-dammed lakes were identified in the Chenab basin (Supplementary Table S15). Moraine-dammed lakes are dominant for glacier-fed type, comprising an area of 4.75 ± 0.18 km^2 (~79% of the total glacier-fed area; Figure 7B), while bedrock-dammed lakes are mostly non-glacier fed types (Figure 7C).

The mean size of the glacial lakes is 0.024 km^2, and the largest glacial lake in the basin is the Samudri Tapu (L396; 1.52 ± 0.03 km^2). The 0.001–0.002 km^2 size class comprises 106 lakes with a total area of 0.15 ± 0.06 km^2 (Figure 7D,E). The maximum number of lakes (166 or ~39%) lies in the 0.002–0.01 km^2 size class, comprising an area of 0.90 ± 0.17 km^2 (~9% of the total area). About 45% of the total lakes are below <0.05 km^2 in size, and comprise only an area of 4% (Figure 7D,E); however, remaining lakes, i.e. those >0.05 km^2 in size constitute ~96% of the total lake area. The size class >0.1 km^2 comprises only ~3% (12) of total lakes but encompasses the maximum area of ~49% (4.84 ± 0.12 km^2).

The glacial lakes are distributed in an elevation range between 3390 and 5417 m asl. with a mean elevation of ~4600 m asl. Elevation-dependent distribution of lakes shows an inverse relation between number and area (Figure 7F). The elevation zone of 3900–4500 m asl comprises the highest number (154 or ~37%) and surface area (7.29 ± 0.36 km^2 or ~73% of total area). About 49% of the total glacial lakes are below the mean elevation of 4600 m asl and comprise an area of 8.35 ± 0.45 km^2 (~84% of the total area); however, remaining lakes, i.e. those > 4600 m asl constitute only ~16% of the area.

East-west (longitude) and north-south (latitude) distribution depict that larger lakes are on the eastern side of the Chenab basin (Figure 7G). Most of the eastern-side lakes are glacial-fed compared to the glacial-unconnected lakes in the western sector. The maximum density of the glacial lakes in the study area is ~18 glacial lakes per 100 km^2.

4.2. Expansion and temporal changes

In this study, we selected 42 glacial lakes with an area ≥0.05 km^2 in 2022 for GLOF susceptibility assessment. Thus, their surface area changes between 1990 and 2022 were examined (Table 4; Figure 8). The results show that 21 out of 42 lakes remained unchanged during the observation period (Figure 8). Two lakes (L185 and L218)

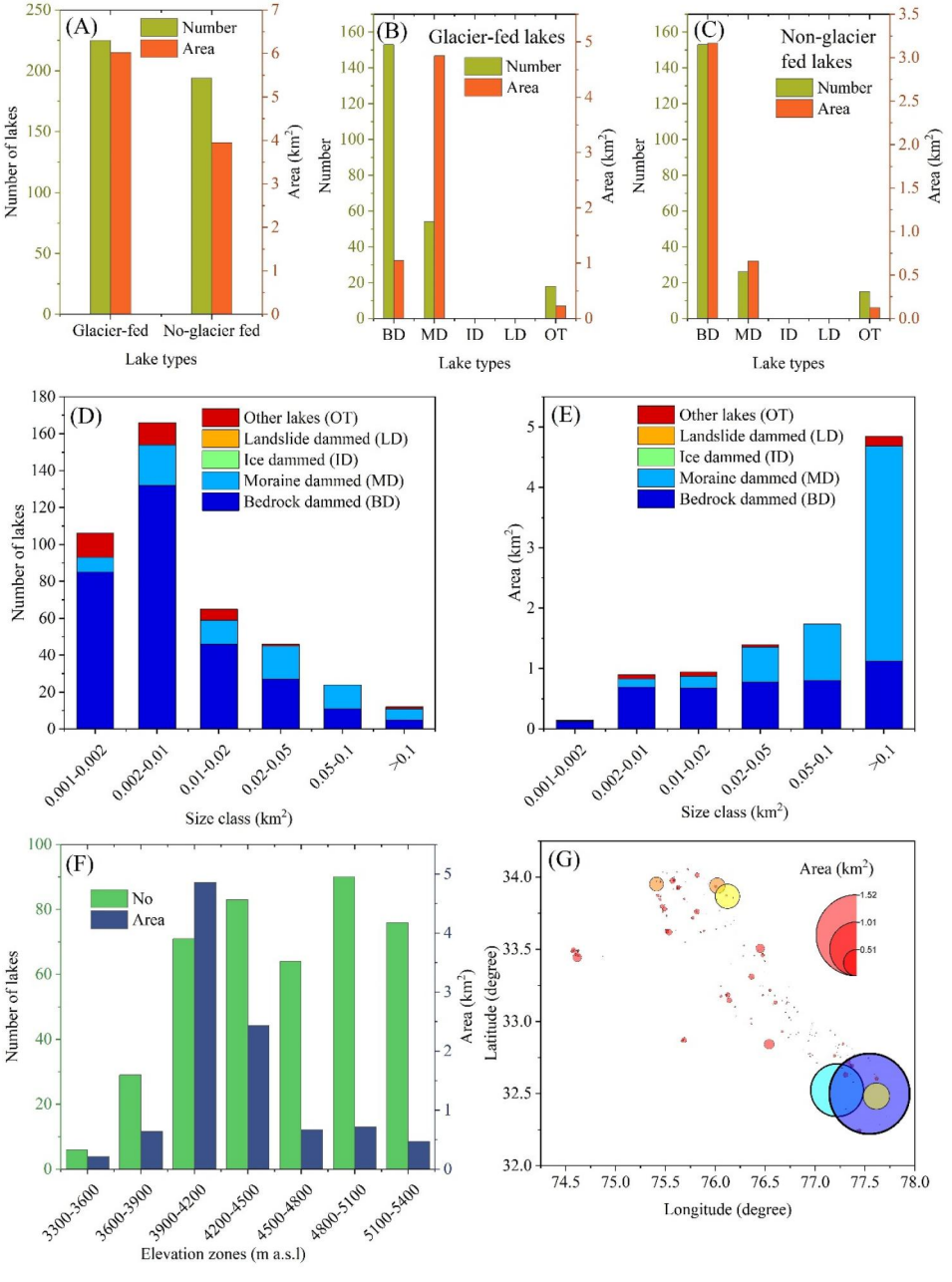

Figure 7. Inventory and statistics of glacial lakes (>0.001 km^2) in the Chenab basin as of 2022. (A) Number and area distribution according to types, (B) Morphology-based distribution of glacier-fed lakes, (C) Morphology-based distribution of non-glacier fed lakes, (D) Number of lakes according to size class and types, (E) Area of lakes according to size class and type, (F) Elevation zone wise distribution, (G) Latitude and longitude wise distribution based on size class.

Table 4. Glacial lakes (>0.05 km^2) with GLOF susceptibility rank in the Chenab basin.

			Area (km^2)				
Lake ID	Long (°)	Lat (°)	1990	2022	Change (%)	Susceptibility index	GLOF class
L147	76.121	33.868	0.223	0.459	51	0.714	Very high
L339	77.221	32.527	0.371	0.997	63	0.665	Very high
L396	77.546	32.497	0.514	1.519	66	0.675	Very high
L415	77.618	32.604	0.027	0.063	57	0.655	Very high
L185	76.363	33.312	0.000	0.102	100	0.556	High
L331	77.195	32.762	0.023	0.053	57	0.615	High
L358	77.307	32.630	0.024	0.092	74	0.588	High
L022	75.447	33.845	0.037	0.047	21	0.526	Moderate
L034	75.492	33.780	0.007	0.082	92	0.523	Moderate
L123	76.019	33.941	0.053	0.297	82	0.522	Moderate
L218	76.539	32.842	0.000	0.182	100	0.545	Moderate
L228	76.602	33.133	0.004	0.067	94	0.496	Moderate
L357	77.280	32.845	0.016	0.047	66	0.450	Moderate
L379	77.373	32.693	0.065	0.065	0	0.453	Moderate
L001	74.569	33.486	0.061	0.061	0	0.329	Low
L002	74.579	33.496	0.087	0.087	0	0.313	Low
L004	74.602	33.468	0.056	0.056	0	0.367	Low
L006	74.614	33.445	0.160	0.160	0	0.411	Low
L011	74.626	33.458	0.047	0.047	0	0.313	Low
L015	75.411	33.952	0.267	0.267	0	0.356	Low
L017	75.422	33.873	0.050	0.059	15	0.376	Low
L028	75.465	33.799	0.065	0.077	15	0.274	Low
L040	75.514	33.625	0.077	0.077	0	0.382	Low
L045	75.537	33.619	0.108	0.108	0	0.420	Low
L047	75.573	33.974	0.101	0.101	0	0.338	Low
L072	75.628	33.932	0.075	0.075	0	0.376	Low
L073	75.632	33.922	0.024	0.048	50	0.383	Low
L077	75.669	32.867	0.054	0.054	0	0.284	Low
L083	75.688	32.872	0.071	0.092	23	0.311	Low
L095	75.774	33.718	0.052	0.052	0	0.315	Low
L099	75.815	33.761	0.096	0.096	0	0.338	Low
L100	75.819	34.015	0.083	0.083	0	0.343	Low
L119	76.004	33.936	0.052	0.052	0	0.401	Low
L126	76.056	33.174	0.027	0.046	41	0.256	Low
L148	76.125	33.184	0.079	0.079	0	0.401	Low
L150	76.139	33.147	0.096	0.096	0	0.328	Low
L195	76.450	33.507	0.160	0.160	0	0.405	Low
L203	76.474	33.460	0.066	0.066	0	0.288	Low
L230	76.672	32.930	0.024	0.047	48	0.431	Low
L362	77.330	32.723	0.016	0.093	83	0.431	Low
L387	77.448	32.245	0.008	0.058	85	0.412	Low
L414	77.615	32.483	0.492	0.492	0	0.410	Low

evolved after 2000, the remaining 19 lakes showed varying change rates ranging from 15 to 85%. The total area of glacial lakes in 1990 was 3.92 ± 0.58 km^2, which expanded by ~75%, reaching 6.86 ± 0.25 km^2 in 2022. On the decadal scale, lake area change was maximum during 2000–2015 (1.84 ± 0.23 km^2; ~0.12 km^2 yr^{-1}), followed by 2015–2022 (0.82 ± 0.12 km^2; ~0.12 km^2 yr^{-1}) and 1990–2000 (0.28 ± 0.20 km^2; ~0.03 km^2 yr^{-1}). Decadal area changes for 42 lakes are provided in Supplementary Table S16. The 10 typical glacial lakes (L387, Samudri Tapu, Gepang Gath, Panchi Nala, L218, L228, L185, L123, L147 and L034) connected with their parent glaciers expanded the most in the basin (Figure 9). L218 emerged after 2013 and experienced a significant increase in size from 0.03 (2015) to 0.18 km^2 (2022), at a rate of ~56% growth per year. Most of the glacial-unconnected lakes showed very little or no

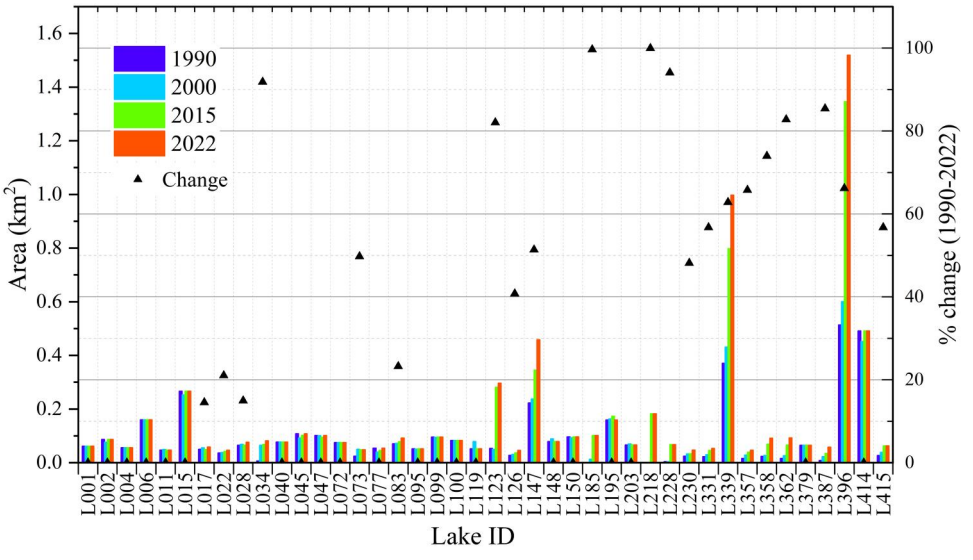

Figure 8. Temporal changes in area of 42 lakes (>0.05 km^2) in the Chenab basin between 1990 and 2022.

growth during the observation period, compared to the glacial-fed lakes in the basin (Figure 9).

4.3. GLOFs susceptibility and sensitivity analysis

The GLOF susceptibility assessment shows that out of 42 glacial lakes assessed, four were classified with very high GLOF susceptibility (Figure 10; Table 4). Similarly, three glacial lakes were classified with high, 7 with moderate, and 28 with low GLOF susceptibility (Figure 10; Table 4). Our method ranked notable glacial lakes like L396 (Samudri Tapu), L339 (Gepang Gath), L415, and L147 as very high GLOF susceptibility. We ranked two other glacial-connected lakes (L358: Kaorang Nala and L185) as highly susceptible. The details on 42 glacial lakes with their susceptibility classes are presented in Table 4.

Our findings revealed that GLOF susceptibility assessment is sensitive to changes in thresholds of class/alternatives of factors. The sensitivity analysis based on shifting of class/alternatives revealed that 42% of the lakes (out of 42) changed their susceptibility class between high and very high when the class/alternative level of F8 is shifted, revealing that mass movement probability is the most sensitive parameter, among others (Supplementary Table S13). Similarly, the number of lakes in the very high class increased from 10 to 19% when the class level of F5 was shifted. Thus, assigning maximum AHP weight to F8 and F5 is justified in the present analysis. No change was observed in the very high GLOF class when F9 and F10 were altered (Supplementary Table S13). The sensitivity analysis based on altering GLOF susceptibility class showed that if the susceptibility class is decreased by 0.05 then two high GLOF class lakes (L331, L354) will be classified into very high class and five moderate GLOF class lakes (L218, L022, L034, L123, L228) will be classified into high class.

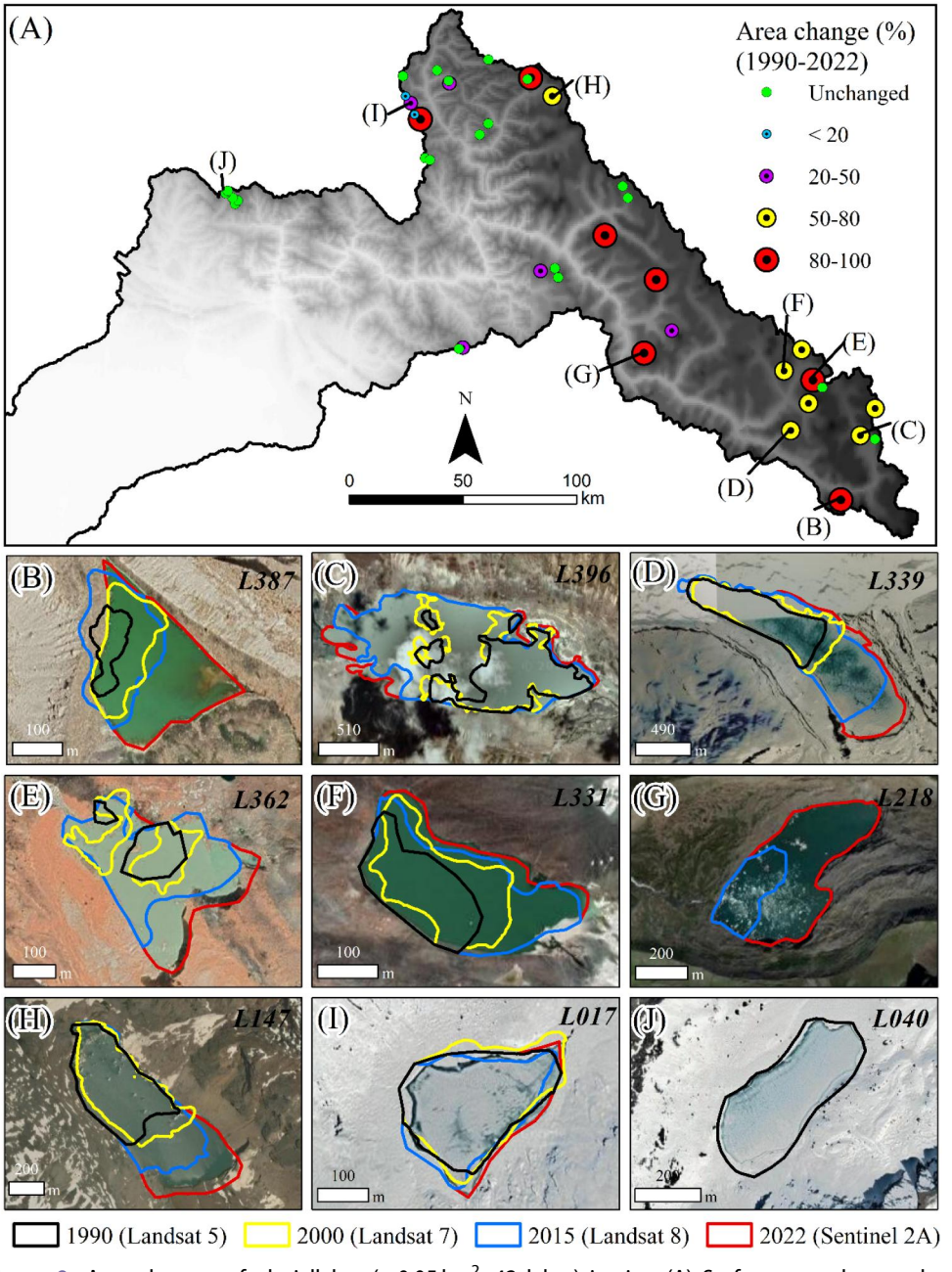

Figure 9. Area changes of glaciallakes (>0.05 km^2; 42 lakes) in size. (A) Surface area change class, (B–J) examples of surface area change of selectedlakes between 1990 and 2022.

Similarly, if the susceptibility class is increased by 0.05, three (L369, L339, L315) out of four very high lakes (Table 4) will fall into the high class (Supplementary Table S14). This shows that the lakes are very sensitive to the small change in GLOF class.

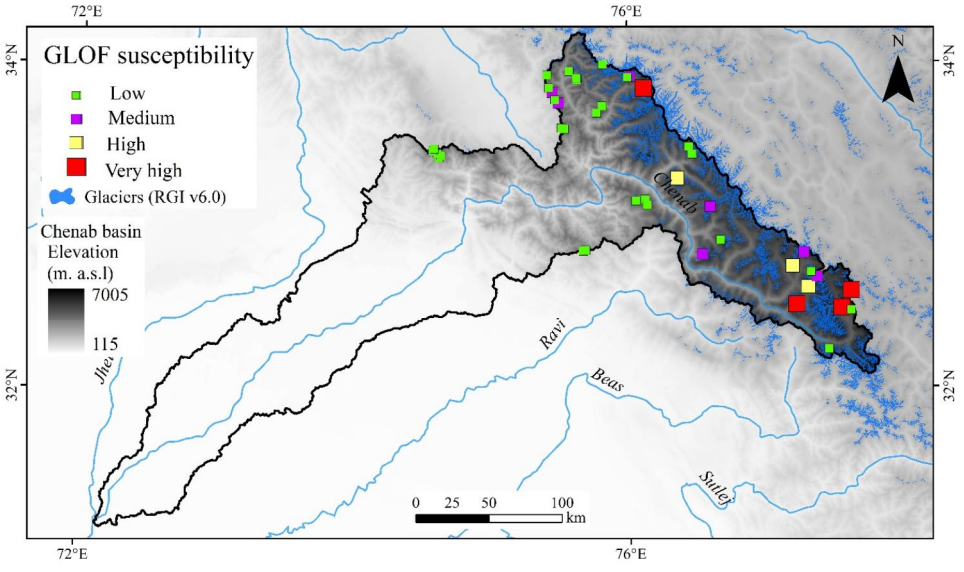

Figure 10. Spatial distribution of 42 glacial lakes assessed with their GLOF susceptibility classes in the Chenab basin.

5. Discussion

5.1. Mapping and inventory of glacial lakes

Glacial lake mapping uncertainty usually results from the data quality (i.e. spatial resolution) used for mapping and other factors such as cloud coverage and seasonal snow (Hanshaw and Bookhagen 2014; Rinzin et al. 2023). Our uncertainty range (~6.92% of total area) is lower than the previously reported studies across the region, which used Landsat images (i.e. ± 16.13% in Zhang et al. 2015), ±13.15% in Wang et al. 2020a), ±30% in Khadka et al. 2018), ±15.96% in Nie et al. 2017)). Present uncertainty (±6.92%) is similar to uncertainty reported in the Bhutan Himalaya (±5.02%) using Sentinel 2 image (Rinzin et al. 2021). We compared the surface area of randomly selected 20 lakes mapped from high-resolution (<1 m) imagery available in GE. Results show an area deviation of < 1% between GE and Sentinel images. The lake mapping from 10 m Sentinel 2 images yielded better results with lower errors than those mapped from 30 m Landsat images because the standard way of detecting an error in lake delineation depends upon the spatial resolution of the images used (Salerno et al. 2012). Our results could even be better if the studies had been performed with data at even higher resolution. Apart from this, ASTER DEM with 30 m coarse resolution was used for extracting and measuring moraine dam geometry and terrain processing. Very detailed information is not possible from these DEM datasets (Khadka et al. 2021; Rinzin et al. 2021).

We followed standard approaches to generate glacial lakes inventory in the Chenab basin. Our 2022 inventory was compared with existing inventories for the Himalayan region (Shugar et al. 2020; Wang et al. 2020a; Chen et al. 2021; Zheng et al. 2021), despite significant variations in mapping time and minimum threshold size (Table 5).

Table 5. Comparison of the number and area of glacial lakes in the Chenab basin with the findings of previous studies.

Source	Study area	Study year	No of lakes	Area of lakes (km^2)	Minimum size (km^2)
This study	Chenab basin	2022	419	9.97 ± 0.69	0.001
This study			223	9.48 ± 0.61	0.0054
This study			165	9.09 ± 0.58	0.0085
This study			36	6.58 ± 0.05	0.05
Wang et al. (2020a)	HMA	2018 ± 2	67	6.08	0.0054
Chen et al. (2021)	HMA	2017 ± 2	63	5.24	0.0085
Shugar et al. (2020)	Worldwide	2015-2018	18	4.14	0.05

HMA = High Mountain Asia.

The number and total area of glacial lakes identified in our study exceeded those in previous studies. By increasing the minimum mapping threshold size to 0.0054 km^2 as of Wang et al. (2020a), the number and area change to 223 and 9.48 ± 0.61 km^2 as of 2022. On the other hand, considering the minimum threshold size of 0.0085 km^2 as of Chen et al. (2021), the glacial lake number and area change to 165 and 9.09 ± 0.58 km^2, respectively in the present study (Table 5). These differences could be attributed to (1) differences in image acquisition, (2) differences in minimum threshold size, and (3) mapping error. The comparison indicates that the earlier inventories have missed glacial lakes, especially in the smaller size ranges, and implies that our study provides a more robust (both qualitative and quantitative) representation of the glacial lake census in the Chenab basin than previous studies at the regional scale. We observed the dominance of small glacial lakes (<0.05 km^2) in the Chenab basin, which is in consonance with previous records (Bhambri et al. 2018), and the general distribution pattern of glacial lakes in the Himalayas (Zhang et al. 2015; Khadka et al. 2018). However, glacial lakes in the larger size categories represent the major portion of the total area, in agreement with earlier findings in the Himalayas (Nie et al. 2017).

5.2. Expansion of glacial Lakes

Glacier recession has led to an increasing number and areal extent of glacial lakes in the majority of high mountain regions all around the world (Nie et al. 2017; Shugar et al. 2020; Veh et al. 2020; Zheng et al. 2021). Between 1990 and 2015, Nie et al. (2017) reported an expansion rate of ~14.1% in the Himalayan region. Wang et al. (2020a) reported an average rate of increase in area of ~15.2% during 1990–2018. Heterogeneous expansion rates have been reported in Nepal (~30%; Khadka et al. 2018), and Bhutan Himalaya (~20%; Rinzin et al. 2021). A similar pattern is observed in the Chenab basin (Kumar et al. 2017; Prakash and Nagarajan 2017; Das et al. 2023a). Many lakes came into existence in different periods after 1990 and were growing at different expansion rates over the last 30 years in the Chenab basin. Glaciers in the Chenab basin experienced an accelerated areal reduction (Das and Sharma 2019; Das et al. 2023a), and elevation change (Das et al. 2022) at heterogeneous rates across the sub-basin scales. In the Chandrabhaga basin, several studies have reported a significant increase in the number and area of glacial lakes (Prakash

and Nagarajan 2017; Bhambri et al. 2018; Das et al. 2023a). Increasing trends in temperature and declining precipitation may result in rapid deglaciation and the expansion of lakes in the region (Das et al. 2023a). Continued glacier retreat may lead to further expansion and formation of lakes with higher outburst susceptibility and associated GLOF hazards in the basin.

Non-glacier-fed lakes in the basin remain mostly unchanged (Figure 9). These lakes dominate the western part of the basin, primarily comprising the Pir-Panjal range where precipitation mostly occurs in liquid form during the monsoon season (Ali et al. 2021; Padder et al. 2022). Our findings are consistent with regional-scale studies in the Himalayas, which have reported either a minor shift in the trajectory of non-glacier-fed lakes since 1990 (Zhang et al. 2015) or a relatively stable situation (Nie et al. 2017).

On the other hand, maximum expansion was observed for glacier-fed lakes compared to non-glacier-fed lakes, which aligns with earlier findings for the entire Himalayan region (Zhang et al. 2015; Aggarwal et al. 2017; Nie et al. 2017; Khadka et al. 2018; Wang et al. 2020a; Rinzin et al. 2021). The differences in expansion rates between non-glacier-fed and glacier-fed lakes can be explained by considering the sources of water for the lakes. When a lake is no longer in contact with its parent glacier, the only water source is the drainage of meltwater from upstream seasonal snow and precipitation. In contrast, a lake in contact with a glacier receives additional water from subglacial melting and calving of the glacier front into the lake (Gardelle et al. 2011). Lakes attached to glaciers are inclined towards faster surface area expansion due to a positive feedback mechanism between the lake and ice (Carrivick and Tweed 2013; Tweed and Carrivick 2015; King et al. 2018).

Most of the large lakes in the Chenab basin are glacier-fed, depicting the maximum rate of areal expansion. Similar scenarios have been reported worldwide, including Bhutan (Ageta et al. 2000; Rinzin et al. 2021), Nepal (ICIMOD 2011; Rounce et al. 2016, 2017; Haritashya et al. 2018; Khadka et al. 2018, 2021), and Alps (Huggel et al. 2002) and Andes (Hanshaw and Bookhagen 2014; Iribarren Anacona et al. 2018; Kougkoulos et al. 2018).

5.3. GLOF hazard potential

5.3.1. GLOF susceptibility factors and weightage

The initial step in GLOF mitigation and early warning preparation involves assessing the hazard potential of glacial lakes. In this study, we utilized 10 factors to identify PDGLs and employed multiple-criteria decision-making techniques to generate a hazard-potential ranking for 42 glacial lakes $>0.05\,km^2$ in size. The Himalayan region has been documented as a hotspot of GLOF (Westoby et al. 2014b; Nie et al. 2018). More than 60 GLOFs have been reported; however, only a few have been recorded with detailed information (Nie et al. 2018). The details and exact triggering factors of GLOFs are still difficult to obtain for all outburst cases. Existing studies to understand the GLOF triggering factors heavily relied on old documents/geomorphological analysis (Nie et al. 2018) and were restricted by the limited explanation of the lake failure process (Veh et al. 2019). Based on Nie et al. (2018), out of 62 historical

GLOF events from the Himalayas, most of them occurred in the central (33) and eastern (29) parts, while no GLOF was reported from the western part (Supplementary Figure S6). In order to validate our findings, we performed a susceptibility assessment on several lakes which had experienced GLOFs in the past. Recent studies (Lützow et al. 2023; Shrestha et al. 2023) provide a comprehensive inventory of historical GLOFs across the Himalayan region. Based on heterogeneous morphological and topographical settings, we randomly assessed and compiled datasets for 13 glacial lakes (Table 6). We observed GLOF susceptibility index values between 0.43 and 0.80. Out of these 13 lakes, nine fell in the very high and three in the high GLOF susceptibility category. Only one lake was in the medium susceptibility category. These findings established that our GLOF susceptibility method was robust enough to use on the other lakes in the Chenab basin.

Although there are technical guidelines for assessing glacier and permafrost-related hazards in mountain regions, published by the International Association of Cryospheric Sciences and the International Permafrost Association Standing Group on Glacier and Permafrost Hazards (Allen et al. 2017), there is currently no standard scheme for assessing lake hazards (Racoviteanu et al. 2022). The existing schemes (i.e. Wang et al. 2011; Worni et al. 2013; Iribarren Anacona et al. 2014; Rounce et al. 2016; Aggarwal et al. 2017; Kougkoulos et al. 2018; Dubey and Goyal 2020; Khadka et al. 2021; Rinzin et al. 2021) for ranking glacial lake hazards, differ in terms of the parameters utilized, the weight allocated to each parameter, and the data sources (field/remote sensing/a priori knowledge) (Emmer and Vilímek, 2013; Rounce et al. 2016). Moreover, these schemes often fail to parameterize crucial GLOF processes (Racoviteanu et al. 2022). Analysing all the factors associated with past GLOFs in the Himalayan region and identifying key parameters and thresholds governing the outburst is a formidable challenge in the present study. The factors used in the present study might not be applicable to all GLOFs in the Himalayas; instead, they are focused on the study area. We summarized the potential GLOF susceptibility factors reported in the Himalayan region (Supplementary Table S4) and selected the 10 most weighted factors (Table 2). The common GLOF-triggering factors in the Himalayas include mass movement (ice, snow, upper flood, precipitation, and/or rock) entering the lake (Worni et al. 2013; Westoby et al. 2014a; Das et al. 2015; Nie et al. 2018; Zhang et al. 2022) and subsequently overtopping and eroding the moraine (Rounce et al. 2016). Other factors may include the destruction of dam due to hydrostatic pressure and pipping (Westoby et al. 2014a; Rounce et al. 2016; Nie et al. 2018), seismic activity-related slope failure (Ives et al. 2010; Osti et al. 2011; ICIMOD 2011; Byers et al. 2019) and cloudburst events (Das et al. 2015). The precise reasons behind many outburst floods remain elusive due to a dearth of in-situ observations. Integrating field investigations with remote sensing datasets will become progressively crucial in uncovering the triggers and processes behind GLOF events.

We present an assessment of GLOF susceptibility for lakes in the Chenab basin, an area for which glacial lake dynamics have not been previously investigated. In our study, Samudri Tapu and Gepang Gath lakes were classified as very high in susceptibility, with mass movement assigned the maximum weight, similar to the findings of Prakash and Nagarajan (2017). Glacial lakes larger in size and prone to mass

Table 6. Characteristics and outburst susceptibility scores of several well-known glacial lakes and GLOF events in the Himalayan-Tibetan region.

Date	Region	Lat (°)	Long (°)	Lake name[a]	Area (km^2)[b]	Expansion rate (%)[b]	Glacier-lake distance (m)[c]	Slope glacier-lake (°)	Moraine W-H ratio	Freeboard	Dam distal slope (°)	Mass movement probability	Seismic zone	Cloudburst	Susceptibility index (level)[d]	Triggers	Sources
2001	Tibet China	28.207	89.748	Chongbaxia Tso	0.79	39	0	45	0.5-1	4	60	High	High	Low	0.67 (VH)	Ice avalanche	(Komori et al. 2012; Nie et al. 2020)
17-01-2013	Central Indian Himalaya	30.749	79.061	Chorabari	0.03	< 50	No glacier	N/A	0.1–0.5	>5	35–40	High	High	High	0.62 (H)	Cloudburst	(Das et al. 2015)
04-08-1985	Eastern Nepal	27.874	86.589	Dig Tso	0.50	50–100	0	<12	2.3	0	25–30	High	High	Medium	0.76 (VH)	Ice avalanche	(ICIMOD 2011; Gurung et al. 2017)
07-05-2016	Tibet China	28.078	86.064	Gongbatongsha Co	0.35	59	313	70	> 10	6	< 10	High	High	Medium	0.65 (VH)	Unknown	(Nie et al. 2018)
06-08-2014	Ladakh	33.617	77.614	Gya	0.11	257	0	22	6	0	35	High	Medium	Low	0.80 (VH)	A piping failure of the frontal moraine	(Schmidt et al. 2020; Majeed et al. 2021)
23-05-2002	China Tibet	28.213	85.851	Jialong Co	0.61	145	0	3	3	12	35	High	High	Medium	0.68 (VH)	Ice avalanche, precipitation	(Nie et al. 2018)
20-06-2020	Tibet China	30.356	93.631	Jinwuco Tso	0.56	56	0	30	5	4	48	High	Medium	Low	0.68 (VH)	Debris landslide, extreme climate events	(Zheng et al. 2021)
20-04-2017	Nepal E	27.814	87.141	Langmale	1.70	71	0	<10	> 0.5	<1	< 10	High	High	Med	0.76 (VH)	Rock avalanche, Earthquake	(Byers et al. 2019)
28-06-2015	Bhutan	28.068	89.580	Lemthang Tsho	0.08	46	0	45	2.5	20	30	Medium	Medium	High	0.43 (M)	Upper flood, ice avalanche, earthquake and precipitation	(Gurung et al. 2017)
03-10-2023	Sikkim	27.912	88.193	South Lonak	1.57	40	0	25	14.4	30	35	High	High	High	0.65 (VH)	Moraine collapse on lake	(Sattar et al. 2023); News report[e]
03-09-1998	Eastern Nepal	27.742	86.845	Tam Pokhri	0.45	46	0	40	>10	>5	30–35	High	High	Medium	0.64 (H)	Ice avalanche	(ICIMOD 2011; Gurung et al. 2017)
07-10-1994	Bhutan	28.091	90.303	Luggye Tso	1.12	37	0	15	11	28	48	High	High	Medium	0.63 (H)	Landslide	(Fujita et al. 2008; Gurung et al. 2017)
1997	Sikkim	27.901	88.783	Kongyangmi La Tsho	0.52	92	0	35	30	4	45	High	High	Low	0.70 (VH)	Ice avalanche	(Nie et al. 2018)

[a]Historical GLOF events and other characteristics of these lakes were compiled from previous studies (Nie et al. 2018; Lützow et al. 2023; Shrestha et al. 2023).
[b]Obtained before GLOF occurred.
[c]Zero glacial-lake distance represents the calving glacier on lakes.
[d]GLOF susceptibility index was calculated before GLOF occurred with the method of this study. Hazard levels: VH: Very high; H: High; and M: Medium.
[e]South Lhonak lake GLOF occurred on 3rd October 2023 (https://www.thehindu.com/sci-tech/energy-and-environment/south-lhonak-lake-flood-teesta-dam-climate/article67503729.ece).

movement, such as snow avalanches or rockfalls, were considered very highly hazardous in the region (Prakash and Nagarajan 2017). Mass movement received maximum weightage in our assessment, similar to the other studies in the Himalayas (Nie et al. 2018; Rinzin et al. 2021). In the adjacent Zanskar basin, studies have suggested that the 2014 Gya GLOF event resulted from a piping failure in the frontal moraine (Schmidt et al. 2020; Majeed et al. 2021).

5.3.2. Glacier-lake interaction

The interaction between glaciers and lakes plays a crucial role in future glacier recession and potential lake growth (Carrivick and Tweed 2013). Changes in glacial lakes, such as their growth, can significantly impact both the lake area and its expansion rate, potentially leading to a reclassification of these lakes (Khadka et al. 2021). Consequently, these alterations may induce variations in GLOF susceptibility classes in the future.

Pro-glacial lakes with wide calving fronts exhibit high expansion rates in the Himalayas (Haritashya et al. 2018). Calving processes in proglacial lakes are considered one of the most frequent causes of GLOF from moraine-dammed lakes (Carrivick and Tweed 2013; Zhang et al. 2015; Aggarwal et al. 2017). Studies have reported continuous growth in Gepang Gath Lake (L339; Figure 11A) in the upper Chandra basin since 1970s (Kumar et al. 2017; Kumar et al. 2021), which may lead to further expansion (Gantayat and Ramsankaran 2023) and may result in outburst (Worni et al. 2013; Sattar et al. 2023). Another pro-glacial lake in the Kadu Nala valley (L218; Figure 11B) emerged after 2008 and has experienced significant growth during the last decades (Ali et al. 2023). The presence of high-activity crevasses in the front and floating ice blocks indicate calving activity in glacier-fed lakes in the basin (Figure 11).

In the study area, large ice-calving Gepang Gath and L218 lakes expanded by more than 80% during the observation period. The rapid expansion may increase GLOF susceptibility in two ways: the expanding lakes may extend into areas prone to avalanches, and the volumetric expansion may impact the moraine dam (Sattar et al. 2023). To enhance GLOF hazard assessment, it is recommended to include field-measured lake bathymetry, model possible future lake extents, and conduct volumetric analysis frequently.

5.3.3. Limitation of AHP

We utilized a multi-criteria assessment framework to prioritize glacial lakes with high and very high susceptibility to GLOFs. This method, based on the AHP, is straightforward, systematic, easily implementable, and repeatable (Satty 1990). Our AHP-based approach aligns with existing qualitative and semi-quantitative methodologies (Bolch et al. 2011; Wang et al. 2011; Iribarren Anacona et al. 2014; Aggarwal et al. 2017; Prakash and Nagarajan 2017; Islam and Patel 2020; Khadka et al. 2021; Rinzin et al. 2021; Ahmed et al. 2022). However, it is important to acknowledge its inherent limitations, including subjectivity in expert evaluation and judgment. The weights assigned to each factor in AHP rely on the subjective two-way comparison matrix. To address this, we maintained compatibility and consistency by incorporating many

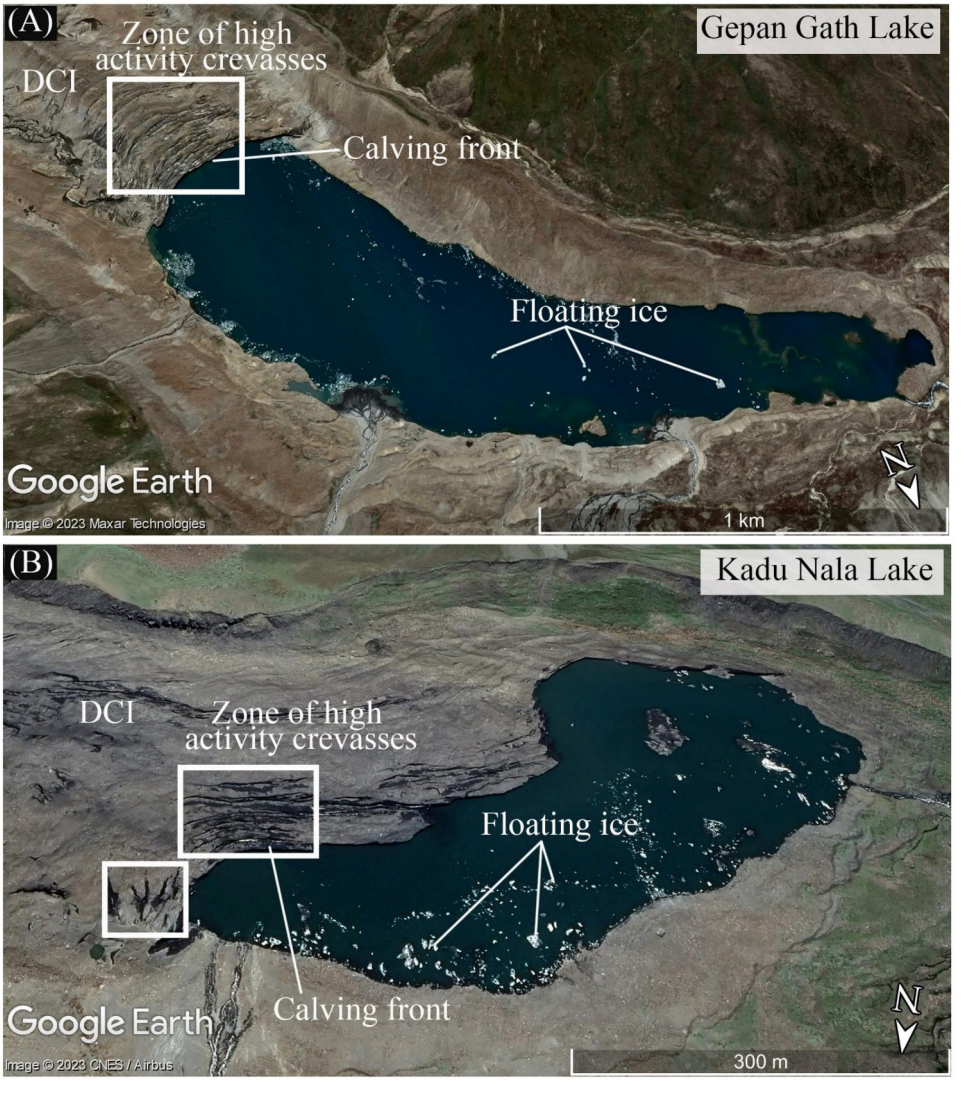

Figure 11. Google earth images (as of 12.09.2019) show the dynamics of glacier-lake interaction for two rapidly growing lakes in the Cheban basin: (A) Gepang Gath lake and (B) Kadu nala lake. DCI: debris-covered ice.

expert opinions in the two-way comparison matrix. It is also crucial to note that the classification of glacial lakes as having high or very high susceptibility does not imply an imminent outburst but underscores the need for prioritized monitoring and thorough ground investigations. While predicting the timing of a potential GLOF is challenging, triggers like snow/ice/rock avalanches and ice-cored moraine degradation heighten the risk of dam collapse (Westoby et al. 2014a; Fischer et al. 2021). Our proposed AHP-based method serves as a preliminary tool for identifying and prioritizing

potentially hazardous lakes at a regional scale, facilitating cost-effective, detailed investigations using readily available datasets.

6. Conclusion

In this study, we established a comprehensive inventory of glacial lakes in the Chenab basin, located in the Western Himalayas, using medium-resolution remote sensing data. A total of 419 lakes $>0.001\,km^2$ were mapped and classified, with 42 lakes having an area $>0.05\,km^2$. The susceptibility of these 42 lakes was assessed using a multi-criterion based AHP framework to assess the degree of outburst susceptibility.

The glacial lake inventory for 2022 indicates a total area of $9.97 \pm 0.69\,km^2$. The total area of the 42 glacial lakes ($>0.05\,km^2$) increased by ~75% between 1990 ($3.92 \pm 0.58\,km^2$) and 2022 ($6.86 \pm 0.25\,km^2$). The study highlights that non-glacier-fed lakes remained nearly stable, while glacier-fed lakes expanded significantly during observation. The results reveal that four lakes are classified as very high, three as high, seven as medium, and 28 as low GLOF susceptibility categories.

Anticipated increases in GLOF hazard in the Chenab basin are attributed to ongoing global warming and glacier recession. Future research should focus on modelling for risk management purposes. High outburst-susceptible lakes require detailed glaciological and geomorphological field surveys to provide high-resolution data for modelling and designing mitigation measures. The study emphasizes the need for a detailed analysis of glacial-lake interaction and geomorphology (i.e. mass movement) in the region to precisely assess GLOF hazard potential and management. This research will help to provide updated and comprehensive information about glacial lakes and their susceptibility to GLOF, contributing to planning and socioeconomic development in the Western Himalayan region.

Acknowledgments

We acknowledge USGS and the European Space Agency for freely providing Landsat and Sentinel images, respectively. Sincere thanks to the editor and three anonymous reviewers for their extremely positive, constructive, and helpful comments on our manuscript, which helped us greatly improve the earlier draft.

Authors contributions

Conceptualization: Suresh Das; Data curation and methodology: Suresh Das, SD and STM; Analysis and original draft: Suresh Das; Writing, Reviewing, and Editing: Suresh Das, MCS, RR; Supervision, and project administration: MCS and RR; Funding: RR. All authors contributed to the final version of the draft.

Disclosure statement

No potential conflict of interest was reported by the author(s).

ORCID

Suresh Das http://orcid.org/0000-0003-4148-8551
Soumik Das http://orcid.org/0000-0002-1368-5438
Sandip Tanu Mandal http://orcid.org/0000-0002-2824-3376
Raaj Ramsankaran http://orcid.org/0000-0001-8602-1934

Data availability statement

Publicly available datasets were analyzed in this study. This data can be found here: Landsat images were obtained from the U.S. Geological Survey (USGS) data portal (https://earthexplorer.usgs.gov/), Sentinel-2 images were downloaded from the Copernicus open access hub of the European Space Agency (https://scihub.copernicus.eu/), ASTER GDEMs were downloaded from Earth data (https://www.earthdata.nasa.gov/), HMA DEMs were obtained from NASA (https://nsidc.org/data/hma_dem8m_mos/versions/1), geological maps were downloaded from Bhukosh website (https://bhukosh.gsi.gov.in/), and earthquake and seismic datasets were downloaded from Earth explorer (https://earthexplorer.usgs.gov/). The datasets generated in this study can be downloaded from https://doi.org/10.5281/zenodo.10477913.

References

Agarwal V, Van Wyk de Vries M, Haritashya UK, Garg S, Kargel JS, Chen YJ, Shugar DH. 2023. Long-term analysis of glaciers and glacier lakes in the Central and Eastern Himalaya. Sci Total Environ. 898:165598. doi: 10.1016/j.scitotenv.2023.165598.

Ageta Y, Iwata S, Yabuki H, Naito N, Sakai A, Narama C, Karma. 2000. Expansion of glacier lakes in recent decades in the Bhutan Himalayas. Debris Covered Glaciers. 264:165–175.

Aggarwal A, Jain SK, Lohani AK, Jain N. 2016. Glacial lake outburst flood risk assessment using combined approaches of remote sensing, GIS and dam break modelling. Geomatics Nat Hazards Risk. 7(1):18–36. doi: 10.1080/19475705.2013.862573.

Aggarwal S, Rai SC, Thakur PK, Emmer A. 2017. Inventory and recently increasing GLOF susceptibility of glacial lakes in Sikkim, Eastern Himalaya. Geomorphology. 295:39–54. doi: 10.1016/j.geomorph.2017.06.014.

Ahmed R, Ahmad ST, Wani GF, Mir RA, Ahmed P, Jain SK. 2022. High resolution inventory and hazard assessment of potentially dangerous glacial lakes in upper Jhelum basin, Kashmir Himalaya, India. Geocarto Int. 37(25):10681–10712. doi: 10.1080/10106049.2022.2038693.

Ali S, Cheema M, Waqas M, Waseem M, Leta M, Qamar M, Awan U, Bilal M, Rahman M. 2021. Flood mitigation in the transboundary Chenab river basin: a basin-wise approach from flood forecasting to management. Remote Sens. 13(19):3916. doi: 10.3390/rs13193916.

Ali SN, Pandey P, Singh P, Mishra S, Shekhar M, Mishra KG, Morthekai P. 2023. Intimidating evidence of climate change from the Higher Himalaya: a case study from Lahaul, Himachal Pradesh, India. J Indian Soc Remote Sens. 51(5):1099–1112. doi: 10.1007/s12524-023-01686-0.

Allen S, Sattar A, King O, Zhang G, Bhattacharya A, Yao T, Bolch T. 2021. Glacial lake outburst flood hazard under current and future conditions: first insights from a transboundary Himalayan basin. Nat Hazards Earth Syst Sci. 22:3765–3785. doi: 10.5194/nhess-2021-167.

Allen SK, Linsbauer A, Randhawa SS, Huggel C, Rana P, Kumari A. 2016. Glacial lake outburst flood risk in Himachal Pradesh, India: an integrative and anticipatory approach considering current and future threats. Nat Hazards. 84(3):1741–1763. doi: 10.1007/s11069-016-2511-x.

Allen S, Frey H, Huggel C. 2017. Assessment of glacier and permafrost hazards in mountain regions-technical guidance document. *International Association of Cryospheric Sciences and*

International Permafrost Association (IACS/IPA) Standing Group on Glacier and Permafrost Hazards (GAPHAZ). doi: 10.13140/RG.2.2.26332.90245.

Allen SK, Zhang G, Wang W, Yao T, Bolch T. 2019. Potentially dangerous glacial lakes across the Tibetan Plateau revealed using a large-scale automated assessment approach. Sci Bull. 64(7):435–445. doi: 10.1016/j.scib.2019.03.011.

Begam S, Sen D. 2019. Mapping of moraine dammed glacial lakes and assessment of their areal changes in the central and eastern Himalayas using satellite data. J Mt Sci. 16(1):77–94. doi: 10.1007/s11629-018-5023-1.

Bhambri R, Misra A, Kumar A, Gupta AK, Verma A, Tiwari SK. 2018. Glacier Lake inventory of Himachal Pradesh. Himalayan Geol. 39(1):1–32.

Bolch T, Buchroithner MF, Peters J, Baessler M, Bajracharya S. 2008. Identification of glacier motion and potentially dangerous glacial lakes in the Mt. Everest region/Nepal using space-borne imagery. Nat Hazards Earth Syst Sci. 8(6):1329–1340. doi: 10.5194/nhess-8-1329-2008.

Bolch T, Peters J, Yegorov A, Pradhan B, Buchroithner M, Blagoveshchensky V. 2011. Identification of potentially dangerous glacial lakes in the northern Tien Shan. Nat Hazards. 59(3):1691–1714. doi: 10.1007/s11069-011-9860-2.

Bookhagen B, Burbank DW. 2006. Topography, relief, and TRMM-derived rainfall variations along the Himalaya. Geophys Res Lett. 33(8):1–5. doi: 10.1029/2006GL026037.

Budhathoki KP, Bajracharya O, Pokharel B. 2010. Assessment of Imja Glacier Lake outburst Flood (GLOF) Risk in Dudh Koshi River Basin using remote sensing techniques. J Hydrol and Meteorol. 7(1):75–91. doi: 10.3126/jhm.v7i1.5618.

Byers AC, Rounce DR, Shugar DH, Lala JM, Byers EA, Regmi D. 2019. A rockfall-induced glacial lake outburst flood, Upper Barun Valley, Nepal. Landslides. 16(3):533–549. doi: 10.1007/s10346-018-1079-9.

Carrivick JL, Tweed FS. 2013. Proglacial Lakes: character, behaviour and geological importance. Quat Sci Rev. 78:34–52. doi: 10.1016/j.quascirev.2013.07.028.

Chen F, Zhang M, Guo H, Allen S, Kargel JS, Haritashya UK, Watson CS. 2021. Annual 30 m dataset for glacial lakes in High Mountain Asia from 2008 to 2017. Earth Syst Sci Data. 13(2):741–766.

Clague JJ, Evans SG. 2000. A review of catastrophic drainage of moraine-dammed lakes in British Columbia. Quat Sci Rev. 19(17-18):1763–1783. doi: 10.1016/S0277-3791(00)00090-1.

Cook SJ, Kougkoulos I, Edwards LA, Dortch J, Hoffmann D. 2016. Glacier change and glacial lake outburst flood risk in the Bolivian Andes. Cryosphere. 10(5):2399–2413. doi: 10.5194/tc-10-2399-2016.

Das S, Kar NS, Bandyopadhyay S. 2015. Glacial lake outburst flood at Kedarnath, Indian Himalaya: a study using digital elevation models and satellite images. Nat Hazards. 77(2):769–786. doi: 10.1007/s11069-015-1629-6.

Das S, Krishna M, Chand M, Saini R, Kumar M, Kumar Pavitra V, Pankaj K. 2023b. Reconstraining the Quaternary glacial history of Lahaul Himalaya, northern India. Quat Sci Rev. 316:108258. doi: 10.1016/j.quascirev.2023.108258.

Das S, Mukherjee J, Bhattacharyya S, Patel PP, Banerjee A. 2022. Detection of groundwater potential zones using analytical hierarchical process (AHP) for a tropical river basin in the Western Ghats of India. Environ Earth Sci. 81(16):1–19. doi: 10.1007/s12665-022-10543-1.

Das S, Sharma MC. 2019. Glacier changes between 1971 and 2016 in the Jankar Chhu Watershed, Lahaul Himalaya, India. J Glaciol. 65(249):13–28. doi: 10.1017/jog.2018.77.

Das S, Sharma MC, Murari MK, Nüsser M, Schmidt S. 2023a. Half-a-century (1971–2020) of glacier shrinkage and climatic variability in the Bhaga basin, western Himalaya. J Mt Sci. 20(2):299–324. doi: 10.1007/s11629-022-7598-9.

Deswal S, Sharma MC, Saini R, Dalal P, Kumar P. 2020. Preliminary results of hybrid bathymetry and GLOF risk assessment for Neelkanth lake, Lahaul Himalaya, India. Curr Sci. 119(9):1555–1557. doi: 10.18520/cs/v119/i9/1555-1557.

Drenkhan F, Huggel C, Guardamino L, Haeberli W. 2019. Managing risks and future options from new lakes in the deglaciating Andes of Peru: the example of the Vilcanota-Urubamba basin. Sci Total Environ. 665:465–483. doi: 10.1016/j.scitotenv.2019.02.070.

Dubey S, Goyal MK. 2020. Glacial Lake outburst flood hazard, downstream impact, and risk over the Indian Himalayas. Water Resour Res. 56(4):1–21. doi: 10.1029/2019WR026533.
Emmer A, Cochachin A. 2013. The causes and mechanisms of moraine-dammed lake failures in the Cordillera Blanca, North American Cordillera, and Himalayas. AUC Geographica. 48(2):5–15. doi: 10.14712/23361980.2014.23.
Emmer A, Klimeš J, Mergili M, Vilímek V, Cochachin A. 2016. 882 lakes of the Cordillera Blanca: an inventory, classification, evolution and assessment of susceptibility to outburst floods. Catena. 147:269–279. doi: 10.1016/j.catena.2016.07.032.
Emmer A, Vilímek V. 2013. Review article: lake and breach hazard assessment for moraine-dammed lakes: an example from the Cordillera Blanca. Nat Hazards Earth Syst Sci. 13(6): 1551–1565. doi: 10.5194/nhess-13-1551-2013.
Emmer A, Vilímek V. 2014. New method for assessing the susceptibility of glacial lakes to outburst floods in the Cordillera Blanca, Peru. Hydrol Earth Syst Sci. 18(9):3461–3479. doi: 10.5194/hess-18-3461-2014.
Falatkova K, Šobr M, Neureiter A, Schöner W, Janský B, Häusler H, Engel Z, Bene V. 2019. Development of proglacial lakes and evaluation of related outburst susceptibility at the Adygine ice-debris complex, northern Tien Shan. Earth Surf Dynam. 7(1):301–320. doi: 10.5194/esurf-7-301-2019.
Fan J, An C, Zhang X, Li X, Tan J. 2019. Hazard assessment of glacial lake outburst floods in Southeast Tibet based on RS and GIS technologies. Int J Remote Sens. 40(13):4955–4979. doi: 10.1080/01431161.2019.1577578.
Fischer M, Korup O, Veh G, Walz A. 2021. Controls of outbursts of moraine-dammed lakes in the greater Himalayan region. Cryosphere. 15(8):4145–4163. doi: 10.5194/tc-15-4145-2021.
Frey H, Huggel C, Chisolm RE, Baer P, McArdell B, Cochachin A, Portocarrero C. 2018. Multi-source glacial lake outburst flood hazard assessment and mapping for Huaraz, Cordillera Blanca, Peru. Front Earth Sci. 6:1–16. doi: 10.3389/feart.2018.00210.
Fujita K, Suzuki R, Nuimura T, Sakai A. 2008. Performance of ASTER and SRTM DEMs, and their potential for assessing glacial lakes in the Lunana region, Bhutan Himalaya. J Glaciol. 54(185):220–228. doi: 10.3189/002214308784886162.
Gantayat P, Ramsankaran R. 2023. Modelling evolution of a large, glacier - fed lake in the Western Indian Himalaya. Sci Rep. 13(1):1840. doi: 10.1038/s41598-023-28144-8.
Gardelle J, Arnaud Y, Berthier E. 2011. Contrasted evolution of glacial lakes along the Hindu Kush Himalaya mountain range between 1990 and 2009. Glob Planet Change. 75(1-2):47–55. doi: 10.1016/j.gloplacha.2010.10.003.
Gouli MR, Hu K, Khadka N, Talchabhadel R. 2023. Hazard assessment of a pair of glacial lakes in Nepal Himalaya: unfolding combined outbursts of Upper and Lower Barun. Geomatics Nat Hazards Risk. 14(1):1–20. doi: 10.1080/19475705.2023.2266219.
Gruber FE, Mergili M. 2013. Regional-scale analysis of high-mountain multi-hazard and risk indicators in the Pamir (Tajikistan) with GRASS GIS. Nat Hazards Earth Syst Sci. 13(11): 2779–2796. doi: 10.5194/nhess-13-2779-2013.
Gurung DR, Khanal NR, Bajracharya SR, Tsering K, Joshi S, Tshering P, Chhetri LK, Lotay Y, Penjor T. 2017. Lemthang Tsho glacial Lake outburst flood (GLOF) in Bhutan: cause and impact. Geoenviron Disasters. 4(1):1–13. doi: 10.1186/s40677-017-0080-2.
Hanshaw MN, Bookhagen B. 2014. Glacial areas, lake areas, and snow lines from 1975 to 2012: status of the Cordillera Vilcanota, including the Quelccaya Ice Cap, northern central Andes, Peru. Cryosphere. 8(2):359–376. doi: 10.5194/tc-8-359-2014.
Haritashya UK, Kargel JS, Id DHS, Leonard GJ, Strattman K, Watson CS, Id DS, Harrison S, Id KTM, Regmi D. 2018. Evolution and controls of large Glacial Lakes in the Nepal Himalaya. Remote Sens. 10(5):798. doi: 10.3390/rs10050798.
Hu J, Yao X, Duan H, Zhang Y, Wang Y, Wu T. 2022. Temporal and spatial changes and GLOF susceptibility assessment of Glacial Lakes in Nepal from 2000 to 2020. Remote Sens (Basel). 14(19):5034. doi: 10.3390/rs14195034.

Huggel C, Haeberli W, Kääb A, Bieri D, Richardson S. 2004. An assessment procedure for glacial hazards in the Swiss Alps. Can Geotech J. 41(6):1068–1083. doi: 10.1139/t04-053.
Huggel C, Kääb A, Haeberli W, Teysseire P, Paul F. 2002. Remote sensing based assessment of hazards from glacier lake outbursts: A case study in the Swiss Alps. Can Geotech J. 39(2): 316–330. doi: 10.1139/t01-099.
ICIMOD. 2011. Glacial lakes and glacial lake outburst floods in Nepal. Kathmandu: ICIMOD.
Immerzeel WW, Beek L, Bierkens MFP. 2010. Climate change will affect the Asian Water Towers. Science. 328(5984):1382–1385. doi: 10.1126/science.1183188.
Iribarren Anacona P, Norton K, Mackintosh A, Escobar F, Allen S, Mazzorana B, Schaefer M. 2018. Dynamics of an outburst flood originating from a small and high-altitude glacier in the Arid Andes of Chile. Nat Hazards. 94(1):93–119. doi: 10.1007/s11069-018-3376-y.
Iribarren Anacona P, Norton KP, Mackintosh A. 2014. Moraine-dammed Lake failures in Patagonia and assessment of outburst susceptibility in the Baker Basin. Nat Hazards Earth Syst Sci. 14(12):3243–3259. doi: 10.5194/nhess-14-3243-2014.
Islam N, Patel PP. 2020. Inventory and GLOF hazard assessment of glacial lakes in the Sikkim Himalayas, India. Geocarto Int. 37(13):3840–3876. doi: 10.1080/10106049.2020.1869332.
Ives JD, Shrestha RB, Mool PK. 2010. Formation of Glacial Lakes in the Hindu Kush-Himalayas and GLOF risk assessment. Kathmandu: ICIMOD.
Jha LK, Khare D. 2017. Detection and delineation of glacial lakes and identification of potentially dangerous lakes of Dhauliganga basin in the Himalaya by remote sensing techniques. Nat Hazards. 85(1):301–327. doi: 10.1007/s11069-016-2565-9.
Kapitsa V, Shahgedanova M, MacHguth H, Severskiy I, Medeu A. 2017. Assessment of evolution and risks of glacier lake outbursts in the Djungarskiy Alatau, Central Asia, using Landsat imagery and glacier bed topography modelling. Nat Hazards Earth Syst Sci. 17(10): 1837–1856. doi: 10.5194/nhess-17-1837-2017.
Kaushik S, Rafiq M, Joshi PK, Singh T. 2020. Examining the glacial lake dynamics in a warming climate and GLOF modelling in parts of Chandra basin, Himachal Pradesh, India. Sci Total Environ. 714:136455. doi: 10.1016/j.scitotenv.2019.136455.
Khadka N, Chen X, Nie Y, Thakuri S, Zheng G, Zhang G. 2021. Evaluation of Glacial Lake outburst flood susceptibility using multi-criteria assessment framework in Mahalangur Himalaya. Front Earth Sci. 8:1–16. doi: 10.3389/feart.2020.601288.
Khadka N, Zhang G, Thakuri S. 2018. Glacial lakes in the Nepal Himalaya: inventory and decadal dynamics (1977-2017). Remote Sens. 10(12):1–19. doi: 10.3390/rs10121913.
Khanal NR, Hu JM, Mool P. 2015. Glacial lake outburst flood risk in the Poiqu/Bhote Koshi/Sun Koshi river basin in the Central Himalayas. Mt Res Dev. 35(4):351–364. doi: 10.1659/MRD-JOURNAL-D-15-00009.
Khanal NR, Mool PK, Shrestha AB, Rasul G, Ghimire PK, Shrestha RB, Joshi SP. 2015. A comprehensive approach and methods for Glacial Lake outburst flood risk assessment, with examples from Nepal and the transboundary area. Int J Water Resour Dev. 31(2):219–237. doi: 10.1080/07900627.2014.994116.
King O, Dehecq A, Quincey D, Carrivick J. 2018. Contrasting geometric and dynamic evolution of lake and land-terminating glaciers in the central Himalaya. Glob Planet Change. 167: 46–60. doi: 10.1016/j.gloplacha.2018.05.006.
Komori J, Koike T, Yamanokuchi T, Tshering P. 2012. Glacial lake outburst events in the Bhutan Himalayas. Glob Environ Res. 16:59–70.
Kougkoulos I, Cook SJ, Edwards LA, Clarke LJ, Symeonakis E, Dortch JM, Nesbitt K. 2018. Modelling glacial lake outburst flood impacts in the Bolivian Andes. Nat Hazards. 94(3): 1415–1438. doi: 10.1007/s11069-018-3486-6.
Kumar L, Parmanand P, Patel LK, Sharma P, Laluraj CM, Thamban M, Singh A, Ravindra R. 2017. A geospatial analysis of Samudra Tapu and Gepang Gath glacial lakes in the Chandra Basin, Western Himalaya. Nat Hazards. 86(3):1275–1290. doi: 10.1007/s11069-017-2743-4.
Kumar V, Mehta M, Shukla T. 2021. Spatially resolved estimates of glacial retreat and lake changes from Gepang Gath Glacier, Chandra Basin, Western Himalaya, India. J Geol Soc India. 97(5):520–526. doi: 10.1007/s12594-021-1718-y.

Linsbauer A, Frey H, Haeberli W, Machguth H, Azam MF, Allen S. 2016. Modelling glacier-bed over deepenings and possible future lakes for the glaciers in the Himalaya-Karakoram region. Ann Glaciol. 57(71):119–130. doi: 10.3189/2016AoG71A627.

Liu M, Chen N, Zhang Y, Deng M. 2020. Glacial lake inventory and lake outburst flood/debris flow hazard assessment after the Gorkha earthquake in the Bhote Koshi Basin. Water. 12(2): 464. doi: 10.3390/w12020464.

Lützow N, Veh G, Korup O. 2023. A global database of historic glacier lake outburst floods. Earth Syst Sci Data. 15(7):2983–3000. doi: 10.5194/essd-15-2983-2023.

Majeed U, Rashid I, Sattar A, Allen S, Stoffel M, Nüsser M, Schmidt S. 2021. Recession of Gya Glacier and the 2014 glacial lake outburst flood in the Trans-Himalayan region of Ladakh, India. Sci Total Environ. 756:144008. doi: 10.1016/j.scitotenv.2020.144008.

Mal S, Allen SK, Frey H, Huggel C, DImri AP. 2021. Sectorwise assessment of Glacial Lake outburst flood danger in the Indian Himalayan Region. Mt Res Dev. 41(1):R1–R12. doi: 10.1659/MRD-JOURNAL-D-20-00043.1.

McKillop RJ, Clague JJ. 2007. Statistical, remote sensing-based approach for estimating the probability of catastrophic drainage from moraine-dammed lakes in southwestern British Columbia. Glob Planet Change. 56(1-2):153–171. doi: 10.1016/j.gloplacha.2006.07.004.

Mergili M, Müller JP, Schneider JF. 2013. Spatio-temporal development of high-mountain lakes in the headwaters of the Amu Darya River (Central Asia). Glob Planet Change. 107: 13–24. doi: 10.1016/j.gloplacha.2013.04.001.

Mergili M, Pudasaini SP, Emmer A, Fischer JT, Cochachin A, Frey H. 2020. Reconstruction of the 1941 GLOF process chain at Lake Palcacocha (Cordillera Blanca, Peru). Hydrol Earth Syst Sci. 24(1):93–114. doi: 10.5194/hess-24-93-2020.

Mergili M, Schneider D, Worni R, Schneider JF. 2011. Glacial lake outburst floods in the Pamir of Tajikistan: challenges in prediction and modelling. International Conference on Debris-Flow Hazards Mitigation: Mechanics, Prediction, and Assessment, Proceedings. 973–982. doi: 10.4408/IJEGE.2011-03.B-106.

Nagai H, Ukita J, Narama C, Fujita K, Sakai A, Tadono T, Yamanokuchi T, Tomiyama N. 2017. Evaluating the scale and potential of GLOF in the Bhutan Himalayas using a satellite-based integral glacier-glacial lake inventory. Geosciences. 7(3):77. doi: 10.3390/geosciences7030077.

Nie Y, Liu Q, Wang J, Zhang Y, Sheng Y, Liu S. 2018. An inventory of historical glacial lake outburst floods in the Himalayas based on remote sensing observations and geomorphological analysis. Geomorphology. 308:91–106. doi: 10.1016/j.geomorph.2018.02.002.

Nie Y, Liu W, Liu Q, Hu X, Westoby MJ. 2020. Reconstructing the Chongbaxia Tsho glacial lake outburst flood in the Eastern Himalaya: evolution, process and impacts. Geomorphology. 370:107393. doi: 10.1016/j.geomorph.2020.107393.

Nie Y, Pritchard HD, Liu Q, Hennig T, Wang W, Wang X, Liu S, Nepal S, Samyn D, Hewitt K, et al. 2021. Glacial change and hydrological implications in the Himalaya and Karakoram. Nat Rev Earth Environ. 2(2):91–106. doi: 10.1038/s43017-020-00124-w.

Nie Y, Sheng Y, Liu Q, Liu L, Liu S, Zhang Y, Song C. 2017. A regional-scale assessment of Himalayan glacial lake changes using satellite observations from 1990 to 2015. Remote Sens Environ. 189:1–13. doi: 10.1016/j.rse.2016.11.008.

Osti R, Bhattarai TN, Miyake K. 2011. Causes of catastrophic failure of Tam Pokhari moraine dam in the Mt. Everest region. Nat Hazards. 58(3):1209–1223. doi: 10.1007/s11069-011-9723-x.

Padder AH, Nandy S, Kothyari GC, Jani C, Lakhote A, Kandregula RS, Joshi N, Taloor AK, Chauhan G, Thakkar MG. 2022. Geomorphometric appraisal for seismic hazard assessment in the Chenab River Basin of the NW Himalayas, India. Geotecton. 56(4):534–563. doi: 10.1134/S0016852122040069.

Petrakov DA, Chernomorets SS, Viskhadzhieva KS, Dokukin MD, Savernyuk EA, Petrov MA, Erokhin SA, Tutubalina OV, Glazyrin GE, Shpuntova AM, et al. 2020. Putting the poorly documented 1998 GLOF disaster in Shakhimardan River valley (Alay Range, Kyrgyzstan/

Uzbekistan) into perspective. Sci Total Environ. 724:138287. doi: 10.1016/j.scitotenv.2020.138287.
Petrov MA, Sabitov TY, Tomashevskaya IG, Glazirin GE, Chernomorets SS, Savernyuk EA, Tutubalina OV, Petrakov DA, Sokolov LS, Dokukin MD, et al. 2017. Glacial lake inventory and lake outburst potential in Uzbekistan. Sci Total Environ. 592:228–242. doi: 10.1016/j.scitotenv.2017.03.068.
Prakash C, Nagarajan R. 2017. Outburst susceptibility assessment of moraine-dammed lakes in Western Himalaya using an analytic hierarchy process. Earth Surf Processes Landf. 42(14):2306–2321. doi: 10.1002/esp.4185.
Prakash C, Nagarajan R. 2018. Glacial lake changes and outburst flood hazard in Chandra basin, North-Western Indian Himalaya. Geomatics Nat Hazards Risk. 9(1):337–355. doi: 10.1080/19475705.2018.1445663.
Racoviteanu AE, Nicholson L, Glasser NF, Miles E, Harrison S, Reynolds JM. 2022. Debris-covered glacier systems and associated glacial lake outburst flood hazards: challenges and prospects. JGS. 179(3):jgs2021-084. doi: 10.1144/jgs2021-084.
Rawat M, Jain SK, Ahmed R, Lohani AK. 2023. Glacial lake outburst flood risk assessment using remote sensing and hydrodynamic modeling: a case study of Satluj basin, Western Himalayas, India. Environ Sci Pollut Res Int. 30(14):41591–41608. doi: 10.1007/s11356-023-25134-1.
Rinzin S, Zhang G, Sattar A, Wangchuk S, Allen SK, Dunning S, Peng M. 2023. GLOF hazard, exposure, vulnerability, and risk assessment of potentially dangerous glacial lakes in the Bhutan Himalaya. J Hydrol. 619:129311. doi: 10.1016/j.jhydrol.2023.129311.
Rinzin S, Zhang G, Wangchuk S. 2021. Glacial Lake area change and potential outburst flood hazard assessment in the Bhutan Himalaya. Front Earth Sci. 9:1–25. doi: 10.3389/feart.2021.775195.
Rounce DR, McKinney DC, Lala JM, Byers AC, Watson CS. 2016. A new remote hazard and risk assessment framework for glacial lakes in the Nepal Himalaya. Hydrol Earth Syst Sci. 20(9):3455–3475. doi: 10.5194/hess-20-3455-2016.
Rounce DR, Watson CS, McKinney DC. 2017. Identification of hazard and risk for glacial lakes in the Nepal Himalaya using satellite imagery from 2000-2015. Remote Sens. 9(7):654. doi: 10.3390/rs9070654.
Salerno F, Thakuri S, D'Agata C, Smiraglia C, Manfredi EC, Viviano G, Tartari G. 2012. Glacial lake distribution in the Mount Everest region: uncertainty of measurement and conditions of formation. Glob Planet Change. 92–93:30–39. doi: 10.1016/j.gloplacha.2012.04.001.
Sattar A, Allen S, Mergili M, Haeberli W, Frey H, Kulkarni AV, Haritashya UK, Huggel C, Goswami A, Ramsankaran RAAJ. 2023. Modeling potential Glacial Lake outburst flood process chains and effects from artificial lake-level lowering at Gepang Gath Lake, Indian Himalaya. JGR Earth Surface. 128(3):1–26. doi: 10.1029/2022JF006826.
Sattar A, Haritashya UK, Kargel JS, Leonard GJ, Shugar DH, Chase DV. 2021. Modeling lake outburst and downstream hazard assessment of the Lower Barun Glacial Lake, Nepal Himalaya. J Hydrol. 598:126208. doi: 10.1016/j.jhydrol.2021.126208.
Satty TL. 1990. Decision making for leaders: the analytic hierarchy process for decisions in a complex world. Pittsburgh: RWS Publication.
Schmidt S, Nüsser M, Baghel R, Dame J. 2020. Cryosphere hazards in Ladakh: the 2014 Gya glacial lake outburst flood and its implications for risk assessment. Nat Hazards. 104(3):2071–2095. doi: 10.1007/s11069-020-04262-8.
Shrestha N. 2020. Detecting multicollinearity in regression analysis. AJAMS. 8(2):39–42. doi: 10.12691/ajams-8-2-1.
Shrestha F, Steiner JF, Shrestha R, Dhungel Y, Joshi SP, Inglis S, Ashraf A, Wali S, Walizada KM, Zhang T. 2023. A comprehensive and version-controlled database of glacial lake outburst floods in High Mountain Asia. Earth Syst Sci Data. 15(9):3941–3961. doi: 10.5194/essd-15-3941-2023.

Shugar DH, Burr A, Haritashya UK, Kargel JS, Watson CS, Kennedy MC, Bevington AR, Betts RA, Harrison S, Strattman K. 2020. Rapid worldwide growth of glacial lakes since 1990. Nat Clim Chang. 10(10):939–945. doi: 10.1038/s41558-020-0855-4.

Shukla A, Garg PK, Srivastava S. 2018. Evolution of glacial and high-altitude lakes in the Sikkim, Eastern Himalaya over the past four decades (1975-2017). Front Environ Sci. 6:1–19. doi: 10.3389/fenvs.2018.00081.

Strozzi T, Wiesmann A, Kääb A, Joshi S, Mool P. 2012. Glacial lake mapping with very high resolution satellite SAR data. Nat Hazards Earth Syst Sci. 12(8):2487–2498. doi: 10.5194/nhess-12-2487-2012.

Tweed FS, Carrivick JL. 2015. Deglaciation and proglacial lakes. Geol Today. 31(3):96–102. doi: 10.1111/gto.12094.

Veh G, Korup O, von Specht S, Roessner S, Walz A. 2019. Unchanged frequency of moraine-dammed glacial lake outburst floods in the Himalaya. Nat Clim Change. 9(5):379–383. doi: 10.1038/s41558-019-0437-5.

Veh G, Korup O, Walz A. 2020. Hazard from Himalayan glacier lake outburst floods. Proc Natl Acad Sci U S A. 117(2):907–912. doi: 10.1073/pnas.1914898117.

Wang S, Che Y, Xinggang M. 2020b. Integrated risk assessment of glacier lake outburst flood (GLOF) disaster over the Qinghai–Tibetan Plateau (QTP). Landslides. 17(12):2849–2863. doi: 10.1007/s10346-020-01443-1.

Wang S, Qin D, Xiao C. 2015. Moraine-dammed lake distribution and outburst flood risk in the Chinese Himalaya. J Glaciol. 61(225):115–126. doi: 10.3189/2015JoG14J097.

Wang W, Yao T, Gao Y, Yang X, Kattel DB. 2011. A first-order method to identify potentially dangerous glacial lakes in a region of the southeastern Tibetan Plateau. Mt Res Dev. 31(2):122–130. doi: 10.1659/MRD-JOURNAL-D-10-00059.1.

Wang X, Guo X, Yang C, Liu Q, Wei J, Yong Z, Liu S, Yanlin Z, Jiang Z, Tang Z. 2020a. Glacial lake inventory of high-mountain Asia in 1990 and 2018 derived from Landsat images. Earth Syst Sci Data. 12(3):2169–2182. doi: 10.5194/essd-12-2169-2020.

Wang X, Liu S, Ding Y, Guo W, Jiang Z, Lin J, Han Y. 2012. An approach for estimating the breach probabilities of moraine-dammed lakes in the Chinese Himalayas using remote-sensing data. Nat Hazards Earth Syst Sci. 12(10):3109–3122. doi: 10.5194/nhess-12-3109-2012.

Wang X, Liu S, Guo W, Xu J. 2008. Assessment and simulation of glacier lake outburst floods for Longbasaba and Pida lakes, China. Mt Res Dev. 28(3–4):310–317. doi: 10.1659/mrd.0894.

Wangchuk S, Bolch T. 2020. Mapping of glacial lakes using Sentinel-1 and Sentinel-2 data and a random forest classification: strengths and challenges. Science of Remote Sensing. 2:100008. doi: 10.1016/j.srs.2020.100008.

Westoby MJ, Glasser NF, Brasington J, Hambrey MJ, Quincey DJ, Reynolds JM. 2014a. Modelling outburst floods from moraine-dammed glacial lakes. Earth Sci Rev. 134:137–159. doi: 10.1016/j.earscirev.2014.03.009.

Westoby MJ, Glasser NF, Hambrey MJ, Brasington J, Reynolds JM, Hassan MAAM. 2014b. Reconstructing historic glacial lakeoutburst floods through numerical modelling and geomorphological assessment: extreme events in the himalaya. Earth Surf Processes Landf. 39(12):1675–1692. doi: 10.1002/esp.3617.

Wilson R, Glasser NF, Reynolds JM, Harrison S, Anacona PI, Schaefer M, Shannon S. 2018. Glacial lakes of the Central and Patagonian Andes. Glob Planet Change. 162:275–291. doi: 10.1016/j.gloplacha.2018.01.004.

Wood JL, Harrison S, Wilson R, Emmer A, Yarleque C, Glasser NF, Torres JC, Caballero A, Araujo J, Bennett GL, et al. 2021. Contemporary glacial lakes in the Peruvian Andes. Glob Planet Change. 204(103574):103574. doi: 10.1016/j.gloplacha.2021.103574.

Wood JL, Harrison S, Wilson R, Emmer A, Kargel JS, Cook SJ, Glasser NF, Reynolds JM, Shugar DH, Yarleque C. 2024. Shaking up assumptions: earthquakes have rarely triggered Andean Glacier Lake outburst floods. Geophys Res Lett. 51(7):e2023GL105578. doi: 10.1029/2023GL105578.

Worni R, Huggel C, Clague JJ, Schaub Y, Stoffel M. 2014. Coupling glacial lake impact, dam breach, and flood processes: A modeling perspective. Geomorphology. 224:161–176. doi: 10.1016/j.geomorph.2014.06.031.

Worni R, Huggel C, Stoffel M. 2013. Glacial lakes in the Indian Himalayas – From an area-wide glacial lake inventory to on-site and modeling based risk assessment of critical glacial lakes. Sci Total Environ. 468-469:S71–S84. doi: 10.1016/j.scitotenv.2012.11.043.

Zhang D, Zhou G, Li W, Han L, Zhang S, Yao X, Duan H. 2023. A robust glacial lake outburst susceptibility assessment approach validated by GLOF event in 2020 in the Nidu Zangbo Basin, Tibetan Plateau. Catena (Amst). 220(PB):106734. doi: 10.1016/j.catena.2022.106734.

Zhang G, Yao T, Xie H, Wang W, Yang W. 2015. An inventory of glacial lakes in the Third Pole region and their changes in response to global warming. Glob Planet Change. 131:148–157. doi: 10.1016/j.gloplacha.2015.05.013.

Zhang T, Wang W, Gao T, An B, Yao T. 2022. An integrative method for identifying potentially dangerous glacial lakes in the Himalayas. Sci Total Environ. 806(Pt 1):150442. doi: 10.1016/j.scitotenv.2021.150442.

Zheng G, Allen SK, Bao A, Ballesteros-Cánovas JA, Huss M, Zhang G, Li J, Yuan Y, Jiang L, Yu T, et al. 2021. Increasing risk of glacial lake outburst floods from future Third Pole deglaciation. Nat Clim Chang. 11(5):411–417. doi: 10.1038/s41558-021-01028-3.